Norwegian University
of Life Sciences

Master's Thesis 2023 30 ECTS
Faculty of Science and Technology

Moment-Resisting Steel Frames Infilled With CLT Panels

Emir Kavara
Structural Engineering and Architecture

Abstract

This thesis investigates the use of CLT-steel hybrid shear walls as seismic force-resisting systems. The system combines the ductility of a steel moment-resisting frame with the stiffness and light weight of CLT panels by using the panels as infills. The design procedure involves determining initial modeling variables, such as the gap between the CLT panel and steel frame, connection configuration, CLT panel thickness and strength, and post-yield stiffness of the steel members.

The response of this seismic force-resisting system was examined at a single-bay, single-story height and compared to a bare steel frame. The study applied a static pushover loading to a nonlinear 3D model of an infilled frame system. Several parametric analyses were performed, such as frame span, connection spacing, panel thickness, and effect of perforations. The results show the effectiveness of the proposed method in controlling horizontal deformation due to seismic forces acting on the hybrid structure.

Table of contents

Abstract iii

Table of contents iv

List of Tables vii

List of Figures viii

Acknowledgments ix

1. Introduction 1

1.1. Background and Personal Motivation 1

1.2. Existing Studies 1

2. Theory 4

2.1. CLT 4

2.1.1. Sustainability 5

2.2. Steel 6

2.3. Hybrid Systems 6

2.4. Connections 7

3. Methodology 8

3.1. Ansys Mechanical APDL 8

3.2. Reference Model 9

3.3. Design Considerations 11

3.3.1. CLT Panel Modeling 11

3.3.2. Steel Frame Modeling 12

3.3.3. Connection Modeling 14

3.3.3.1. COMBIN39 14

3.3.3.2. COMBIN40 16

3.4. Loading 17

3.4.1. Static Pushover Loading 17

3.5. Parametric Analyses 18
3.5.1. Frame Span 19
3.5.2. Connection Spacing 19
3.5.3. Perforations in CLT Panel 20
3.5.4. CLT Panel Thickness 22
4. Results 24
4.1. Reference Model 24
4.2. Parametric Analyses 27
4.2.1. Frame Span 27
4.2.2. Connection Spacing 28
4.2.3. Perforations in CLT Panel 29
4.2.4. CLT Panel Thickness 32
5. Discussion 34
5.1. Limitations 34
5.1.1. Yield Criterion 34
5.1.2. Stress Concentrations and Mesh Size 34
5.2. Reference Model 36
5.3. Comparison With Model in (Dickof, 2013) 37
5.3.1. Modified Yield Stress 39
5.4. Parametric Analyses 40
5.4.1. Frame Span 40
5.4.2. Connection Spacing 42
5.4.3. Perforations in CLT Panel 43
5.4.4. CLT Panel Thickness 44
6. Conclusion 46
6.1. Future Research 47
References 48

Appendices 51

Appendix A Data Points for COMBIN39-Element 51

Appendix B Steel Frame Cross-Sections 52

Appendix C Stress Distribution for Parametric Analyses 53

List of Tables

Table 3.1: Geometric Parameters for the Reference Model 9
Table 3.2: Cross-Section Dimensions of Steel Members 10
Table 3.3: Material Properties of CLT 11
Table 3.4: Material Properties of Steel 13
Table 3.5: Dead Load from Concrete Slab 17
Table 3.6: Frame Spans and Corresponding Connectors for Parametric Analysis 19
Table 3.7: Connection Spacings for Parametric Analysis 20
Table 3.8: Perforations for Parametric Analysis 21
Table 3.9: CLT Panel Properties for Parametric Analysis 23
Table 5.1: Difference in Horizontal Deformation for Reference Model and Model in (Dickof, 2013) 38
Table 5.2: Effect of Increasing Frame Span at a Base Shear of 2500 kN 42
Table 5.3: Effect of Increasing Thickness of CLT Panel at a Base Shear of 2500 kN 45

List of Figures

Figure 2.1: 5-Layer CLT Panel 5
Figure 3.1: Geometry of the Reference Model 10
Figure 3.2: Location of Plastic Hinges 13
Figure 3.3: COMBIN39 Geometry 15
Figure 3.4: Force-Displacement Curve for COMBIN39-Element 16
Figure 3.5: COMBIN40 Geometry 17
Figure 3.6: Gravity and Lateral Load Placement 18
Figure 3.7: Placement of Door Perforation 21
Figure 3.8: Placement of Window Perforations 22
Figure 4.1: Results for the Reference Model 25
Figure 4.2: Von Mises Stress Distribution in Steel Frame – Reference Model 26
Figure 4.3: Von Mises Stress Distribution in CLT Panel – Reference Model 27
Figure 4.4: Results of Parametric Study – Frame Span 28
Figure 4.5: Results of Parametric Study – Connection Spacing 29
Figure 4.6: Results of Parametric Study – Perforations in CLT Panel 30
Figure 4.7: Von Mises Stress Distribution in CLT Panel – Door Perforation 31
Figure 4.8: Von Mises Stress Distribution in CLT Panel – Window Perforations 32
Figure 4.9: Results of Parametric Study – CLT Panel Thickness 33
Figure 5.1: Local Deformation at Top-Left Corner of CLT Panel 35
Figure 5.2: Comparison Between the Reference Model and the Model in (Dickof, 2013) 37
Figure 5.3: Comparison Between the Reference Model and the Model in (Dickof, 2013) With Modified Yield Stress 39

Acknowledgments

I want to sincerely thank my family, whose unwavering support and encouragement were invaluable throughout my academic journey. I would also like to thank the Faculty of Science and Technology at the Norwegian University of Life Sciences for providing me with an excellent learning environment and the resources necessary to complete my master's degree in Structural Engineering and Architecture. I am also grateful to my friends for their companionship and motivation, which helped me overcome my challenges and achieve my goals.

Finally, I extend my heartfelt appreciation to my mentor, Associate Professor Themistoklis Tsalkatidis, whose guidance, expertise, and constructive feedback have been instrumental in shaping my research project and enhancing my professional growth.

Thank you all for being a part of this memorable experience.

1. Introduction

1.1. Background and Personal Motivation

A hybrid shear wall of steel moment-resisting frames with CLT infill is a relatively new concept. Some research studies have been conducted in recent years, but there are still significant shortcomings in the field, highlighted by the lack of production of buildings with such shear walls. Nevertheless, using CLT-steel hybrid systems as shear walls can reshape the construction industry by providing a cost-effective, energy-efficient, and environmentally friendly alternative to conventional building materials and methods.

Timber has a long-standing history in Norway and has been a prominent building material for centuries due to its abundance and durability. In addition, the Norwegian University of Life Sciences is known to have an environmentally friendly and sustainable approach to studies. Therefore, I soon became interested in timber as a building material and its potential for sustainable construction. This curiosity led me to explore using CLT as an alternative to traditional steel and concrete construction methods. The idea of combining CLT with steel moment-resisting frames to create a hybrid structural system that is both seismic-resistant and sustainable intrigued me. I was inspired to investigate this approach further in my master's thesis.

My motivation for this research project is driven by a desire to contribute to developing innovative and sustainable building systems that can withstand the challenges faced by seismic design. Overall, I am excited about this research project's possibilities and hope that my work can contribute to advancing the field of structural engineering in a meaningful way.

1.2. Existing Studies

Although research on the subject is limited, there are quality studies that provide a good foundation for further investigation. The following are some of these studies, highlighted and summarized.

Dickof investigated using CLT panels as infill in a steel moment frame to create a hybrid seismic force-resisting system. The aim was to combine the ductility of steel with the stiffness

and light weight of timber to increase seismic force resistance in regions with moderate to high seismic hazard indices. The thesis included a detailed nonlinear model of a two-dimensional infilled frame system and compared its behavior to that of a similar bare steel frame at three-, six-, and nine-story heights. The results showed that the CLT-steel hybrid system offers improved seismic performance compared to bare steel frames, making it a promising solution for earthquake-prone areas (Dickof, 2013).

Tesfamariam et al. presented a seismic vulnerability assessment of a novel hybrid structure of steel moment-resisting frames and CLT infill panels. The study considered a three-bay, 3-, 6-, and 9-story steel frame structure designed for two ductility levels: ductile and limited ductility. The researchers used OpenSees to perform nonlinear dynamic analysis to study the seismic vulnerability of CLT infilled frames with varying infill configurations (bare frame, one-bay infilled, two-bay infilled, and fully infilled). The results indicated that infilling more bays significantly reduced the structure's fundamental period and seismic vulnerability (Tesfamariam et al., 2014).

Quintana Gallo and Carradine presented a comprehensive review of the current body of research on timber-based hybrid structures. The article examined the advantages and disadvantages of previous research to provide a foundation for upcoming investigations of hybrid timber systems. The report concluded that timber-based hybrid buildings are becoming increasingly popular and require continued research to ensure they are seismically robust, resilient, cost-effective, and sustainable. In addition, further research is needed in areas such as practical methods of dissipating seismic energy, building performance verification, and design guidance to develop code-compliant designs (Quintana Gallo & Carradine, 2018).

Vogiatzis et al. explored the potential of incorporating CLT infill shear walls within steel-framed structures with semi-rigid connections. The study used a three-dimensional finite element model in ANSYS to investigate the mechanical behavior of the single-bay, two-story hybrid system. The results showed that the presence of CLT infill shear walls significantly improved the performance of moment-resisting frame systems in multistory buildings (Vogiatzis et al., 2019).

Khajehpour investigated a hybrid lateral load-resisting system that combined a moderately ductile steel moment-resisting frame with CLT balloon-framed shear walls. The study used various analyses, including linear dynamic, nonlinear static, and nonlinear dynamic analyses, to investigate the proposed hybrid system on 8-, 12-, and 16-story buildings. The results showed that adding a CLT panel to a bare steel frame decreased the maximum drift while the maximum base shear increased (Khajehpour, 2020).

2. Theory

Lateral forces are external loads acting along the height of a structure that causes it to bend, twist, or move sideways. These forces, such as wind and earthquakes, can significantly affect the stability of the structure. Therefore, structures require lateral force-resistance systems to counteract lateral forces and maintain stability.

Shear walls are structural members designed to counteract lateral forces acting on a structure. They transfer lateral forces applied along their height to the ground foundation. Shear walls are crucial in high-rise buildings exposed to lateral wind and seismic forces (Resmi & Roja, 2016). In low-rise buildings, shear walls are vital because there may not be enough structural elements to provide sufficient resistance against lateral forces.

2.1. CLT

Wood has anisotropic properties, meaning its strength varies depending on where and how a load is applied. Various factors influence the strength of wood, including the species and particular characteristics of the tree from which it was sourced. Wood exhibits differing strengths in its three axes, with the highest strength parallel to the grain and the lowest strength perpendicular to it (Stiemer et al., 2012).

Cross-laminated timber (CLT) is a relatively new engineered wood product patented in the mid-90s that has recently gained popularity. It is a plate-shaped product with an odd number of layers, often three, five, or seven. CLT is made by stacking layers of lumber at right angles and gluing them together under pressure. The resulting panel has excellent strength and stiffness, making it suitable for various applications, including walls, floors, and roofs. One of the main reasons why CLT is used in construction is its high stiffness and in-plane bearing capacity. Overall, CLT is an innovative building material with several advantages over traditional construction materials. Its strength, durability, and environmental friendliness make it an attractive option for architects, builders, and developers seeking to create sustainable buildings that are both functional and aesthetically pleasing. CLT's high level of prefabrication also allows for rapid on-site work, usually involving only the assembly and connection of individual panels (Jeleč & Rajčić, 2018). Figure 2.1 shows the cross-section of a 5-layer CLT panel.

Figure 2.1: 5-Layer CLT Panel

Source: Mass Timber Services LTD. (s.a.). *CROSS LAMINATED TIMBER (CLT).* Available at: https://masstimberservices.com/products/clt/ (accessed: 08.05.2023).

2.1.1. Sustainability

Timber construction offers several benefits in terms of sustainability and environmental factors, which has contributed to its increasing popularity in recent years.

Concrete is responsible for 5% of all greenhouse gas (GHG) emissions worldwide. The manufacturing/production of one ton of steel and cement emits 1,5 and 1,1 tonnes of carbon, respectively (Lehmann, 2012). CLT has a lower environmental impact than concrete and steel due to the production of concrete and steel requiring more energy and emitting more greenhouse gases than wood-based materials. Additionally, wood-based materials are renewable resources that can be sustainably harvested, whereas concrete and steel are non-renewable resources that require significant amounts of energy for extraction and processing (Horx-Strathern et al.).

Sustainable forestry, which involves harvesting mature trees and replacing them with samplings, can be argued to reverse CO2 emissions effectively. This is because healthy, growing samplings have a negative CO2 balance. The ability of wood to sequester carbon

removed from the atmosphere makes it an excellent material for buildings, essentially making them large carbon sinks (Horx-Strathern et al.). For example, each ton of produced solid wood panel can sequester up to 1,6 tonnes of CO2 (Lehmann, 2012).

Furthermore, timber is a natural insulator (Horx-Strathern et al.). Therefore, it has low thermal conductivity and can resist heat flow. By retaining the heat within the building, less energy is required for heating. This is particularly beneficial in Norway and other colder counties, as it helps reduce the energy consumption in buildings.

Norway is a country that is naturally rich in wood, and access to it is very high. The use of locally produced materials reduces greenhouse gas emissions from transportation. A local Norwegian producer of GLULAM and CLT uses environmentally certified raw materials from Norway and Sweden (Moelven, s.a.).

2.2. Steel

Unlike wood, steel is an isotropic material with the same mechanical properties in all directions (Khajehpour, 2020). It is a versatile material commonly used in a wide range of construction projects, from high-rise buildings to bridges and industrial facilities. The key characteristics include a high strength-to-weight ratio and high ductility. In addition, steel has high tensile strength, making it suitable for use in systems that experience heavy loads or forces, such as shear walls.

Architects and engineers have long acknowledged the advantages of steel in the construction industry, as evidenced by its consistently high market share over the past two decades. The market share of steel has remained above 90% for single-story industrial buildings and 65% for multistory non-residential buildings. Furthermore, steel is an incredibly sustainable construction material due to its strength, durability, and recyclability without compromising its quality, making it compatible with long-term sustainable development. Disregarding the stated benefits, steel is often chosen based on cost alone. Steel construction offers numerous advantages for all building types and sectors (SteelConstruction.info, s.a.).

2.3. Hybrid Systems

Although a range of research data is available on constructions composed of massive timber, such as laminated veneer lumber (LVL) or CLT, many questions remain unsettled, particularly

when timber is combined with other structural materials (Quintana Gallo & Carradine, 2018). To a certain degree, all timber structures can be considered hybrid structures because steel is primarily used for connections and concrete for foundations. Nevertheless, true hybridization involves combining two or more materials to create a system that utilizes the strength of each material and mitigates its weaknesses (Bhat, 2013).

Combining steel and timber offers several benefits, including enhanced tensile capacity, seismic performance, fire resistance, and cost efficiency. However, different material properties also pose challenges, such as the varying effects of temperature and humidity on steel and timber (Khorasani, 2011).

In addition to steel, timber tends to have a high strength-to-weight ratio, resulting in lighter structures (Slavid, 2005). Because mass and force are proportional during earthquakes, a hybrid system of timber and steel improves seismic performance compared to heavier structures. Steel also enhances the ductility of the system by enabling it to yield and deform without collapse. Ductility is vital in seismic force-resisting systems as it allows for flexing under sudden loads, such as during an earthquake, which dissipates energy (Khorasani, 2011).

2.4. Connections

Connections are critical to hybrid systems because they are crucial in transferring loads between different structural elements and combinations of materials. In moment-resisting steel frames with a CLT infill, the connections must withstand axial and shear forces in perpendicular directions. Therefore, the connections should provide strength and stiffness while allowing for some flexibility to accommodate the differential movement between the two materials.

Ideally, the connections should yield as much as possible with minimum panel crushing (Dickof, 2013). Yielding helps dissipate energy and takes some stress off the CLT panel.

In addition, the connections must account for material incompatibilities. For example, timber and steel behave differently when temperature and moisture change and the connections should allow for material size changes without developing unintended internal stresses (Khorasani, 2011).

3. Methodology

This thesis investigates the effect of adding a CLT panel to a steel moment-resisting frame.

The high in-plane stiffness of the hybrid system will attract additional forces to the frame area. Therefore, it is vital to accurately design the system to maintain structural integrity of both the CLT panel and the frame itself (Vogiatzis et al., 2022). A finite element analysis (FEA) was performed to investigate the behavior of the hybrid seismic force-resisting system.

First, the reference model was analyzed and compared to a bare steel frame. This comparison provided a good sense of the effectiveness of the hybrid system. After that, parametric analyses were performed to provide a deeper understanding of the inner workings of the system and the parameter adjustments that acquire an improved system performance.

3.1. Ansys Mechanical APDL

ANSYS is a widely used computer-aided engineering software that enables engineers to simulate and analyze the behavior of complex physical systems. The program supports various engineering disciplines, including structural mechanics, fluid dynamics, electromagnetics, and systems engineering.

Mechanical APDL (ANSYS Parametric Design Language) is a powerful FEA tool that is one of the ANSYS software products. A key advantage of Mechanical APDL is its code-based approach. Coding enables users to automate complex analyses and perform parametric studies efficiently. Users can write code directly into the program, providing complete control over the analysis process. Alternatively, users can use a menu-driven graphical user interface to perform modeling and analysis tasks.

The program can simulate mechanical and structural engineering problems, including static and dynamic analyses, heat transfer, and fluid-structure interactions. Mechanical APDL is widely used in academic research and industry, providing engineers with a powerful tool for simulating and analyzing complex mechanical systems. The academic version of ANSYS is used for the numerical investigation in this thesis (ANSYS [Computer software], 2022).

3.2. Reference Model

To compare results with (Dickof, 2013), the reference model was modeled as in Chapter 5.1 of the master's thesis mentioned above. The system was modeled as a nonlinear three-dimensional (3D) model. It is a single-story, single-bay construction with geometric parameters as presented in Table 3.1.

Table 3.1: Geometric Parameters for the Reference Model

Parameter	Value
Width	6000 mm
Height	4500 mm
Gap	20 mm
CLT Panel Thickness	99 mm
Column Cross Section	W310x202
Beam Cross Section	W310x143
Maximum Connection Spacing	800 mm

A gap between the CLT panel and steel frame is necessary for construction tolerance and ease of assembly. A conservative gap of 20 mm, also used in (Dickof, 2013), allows for these factors. The CLT panel consists of three timber layers of 33mm thickness, adding up to a total thickness of 99mm. A maximum connection spacing of 800 mm resulted in seven connectors along the height (c/c = 720 mm) and nine connectors along the width (c/c = 702 mm).

Table 3.2 presents the dimensions, while Appendix B visually represents the two considered cross-sections.

Table 3.2: Cross-Section Dimensions of Steel Members

	ID	h [mm]	w [mm]	t_f [mm]	t_w [mm]	A [mm^2]	I_y [mm^4]
Column	W310x202	341	315	31,8	20,1	25800	$520x10^6$
Beam	W310x143	323	309	22,9	14	18200	$347x10^6$

Where:

h	is the height of the cross-section
w	is the width of the cross-section
t_f	is the thickness of the flange
t_w	is the thickness of the web
A	is the area of the cross-section
I_y	is the cross-section's second moment of inertia

Figure 3.1 shows the geometry of the reference model.

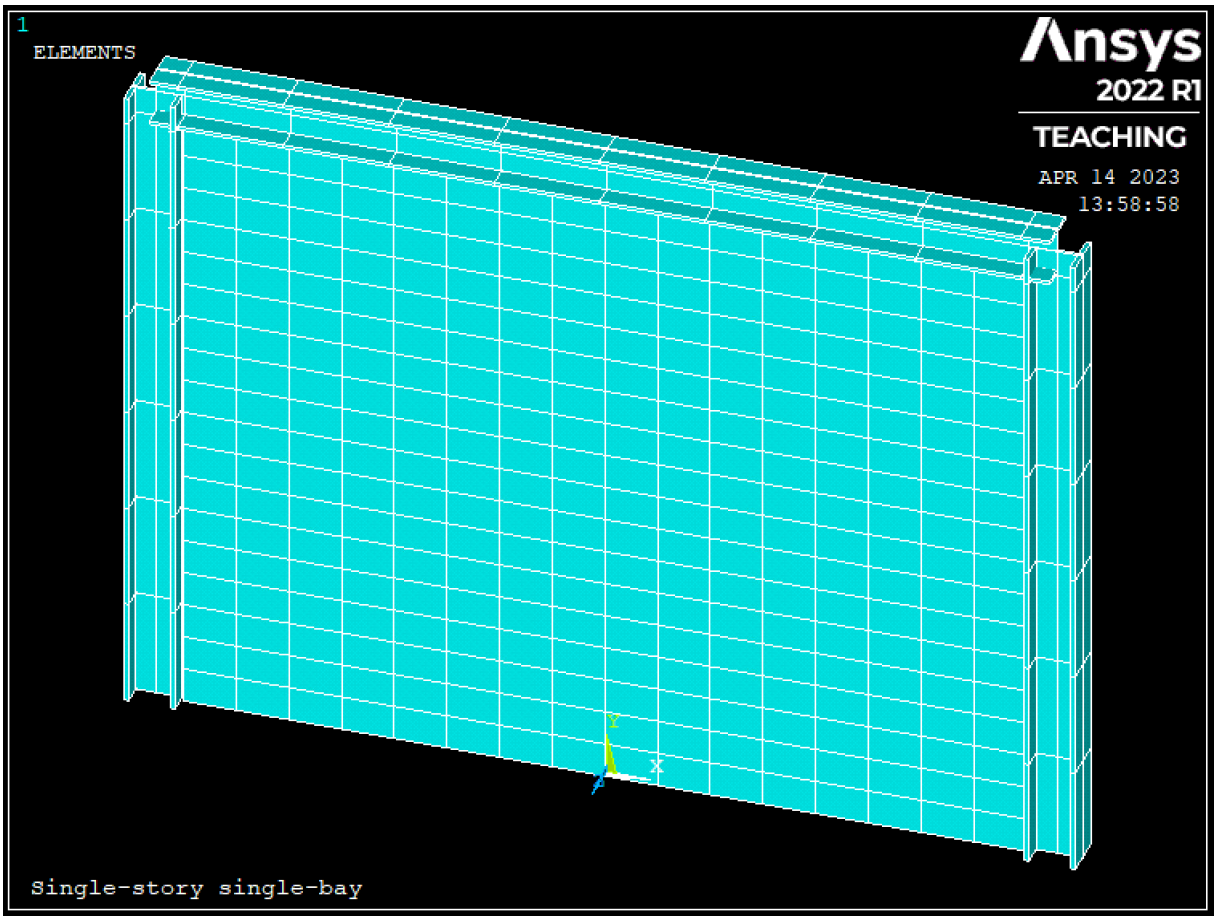

Figure 3.1: Geometry of the Reference Model

3.3. Design Considerations

A computer modeling system is required to perform finite element analysis (FEA) when designing a complex system. FEA uses the input provided about geometry, materials, and loads to represent the system response. Therefore, it is necessary to understand and control the inputs to obtain accurate results, as the program only does what it is asked to do.

Meshing is a critical step in FEA and involves dividing the geometry of a physical system into smaller elements or cells. Meshing can significantly affect simulations' computational time, accuracy, and convergence. The mesh should be refined in areas where the solution varies rapidly or where high levels of accuracy are required. In contrast, the mesh density should be coarser in regions where the solution varies slowly. Proper meshing is essential to obtain accurate and reliable simulation results, making it a crucial aspect of the FEA process.

3.3.1. CLT Panel Modeling

For modeling the CLT panel in ANSYS, SOLSH190 was the selected element type. It is well-equipped to simulate shell structures with various thicknesses (ANSYS, s.a.-e). The panel was assigned bilinear isotropic hardening material properties using the von Mises yield criterion.

The CLT panel is modeled as a single solid panel with isotropic properties instead of several layers of panels that can move relative to each other. The single-panel approach is taken to simplify an otherwise complex problem. The average compressive strength of timber is 17,5 MPa (30 MPa parallel to the grain and 5 MPa perpendicular to the grain). A post-crushing tangent modulus of 10% of the initial modulus of elasticity was used to account for the post-yield stiffness of the panel. Table 3.3 presents a summary of the material properties of CLT.

Table 3.3: Material Properties of CLT

Material	E	ν	f_u	E_p
CLT panel	9,5 GPa	0,46	17,5 MPa	950 MPa

Where:

E	is the modulus of elasticity
v	is Poisson's ratio
f_u	is the crushing strength
E_p	is the post-crushing tangent modulus

The CLT panel mainly acts in compression. However, the wall is not susceptible to buckling, as this topic is beyond the scope of this study. Restraints were placed at each of the four corners of the panel to prevent out-of-plane movement.

3.3.2. Steel Frame Modeling

BEAM189 was the element type selected for the steel frame. The element is well suited for nonlinearly analyzing slender to moderately thick beam structures (ANSYS, s.a.-a). The steel frame was assigned two material profiles: elastic perfectly plastic and linear elastoplastic. The use of each of these is discussed later in this section. In ANSYS, they were both assigned bilinear isotropic hardening material properties using the von Mises yield criterion.

Plastic hinges are the frame regions where plastic deformation occurs. They dissipate energy by allowing the beam to deform in a ductile manner. Plastic hinges are typically used in the beam-to-column connections of moment-resisting frames, where the two members transfer moments. They were designed to accommodate a certain amount of deformation before yielding.

The plastic hinges were placed in the beam-to-column connections with the same length as the spacing between the connectors. This ensures that each steel element's end aligns with the connectors between the frame and the CLT panel. Figure 3.2 shows the location of the plastic hinges.

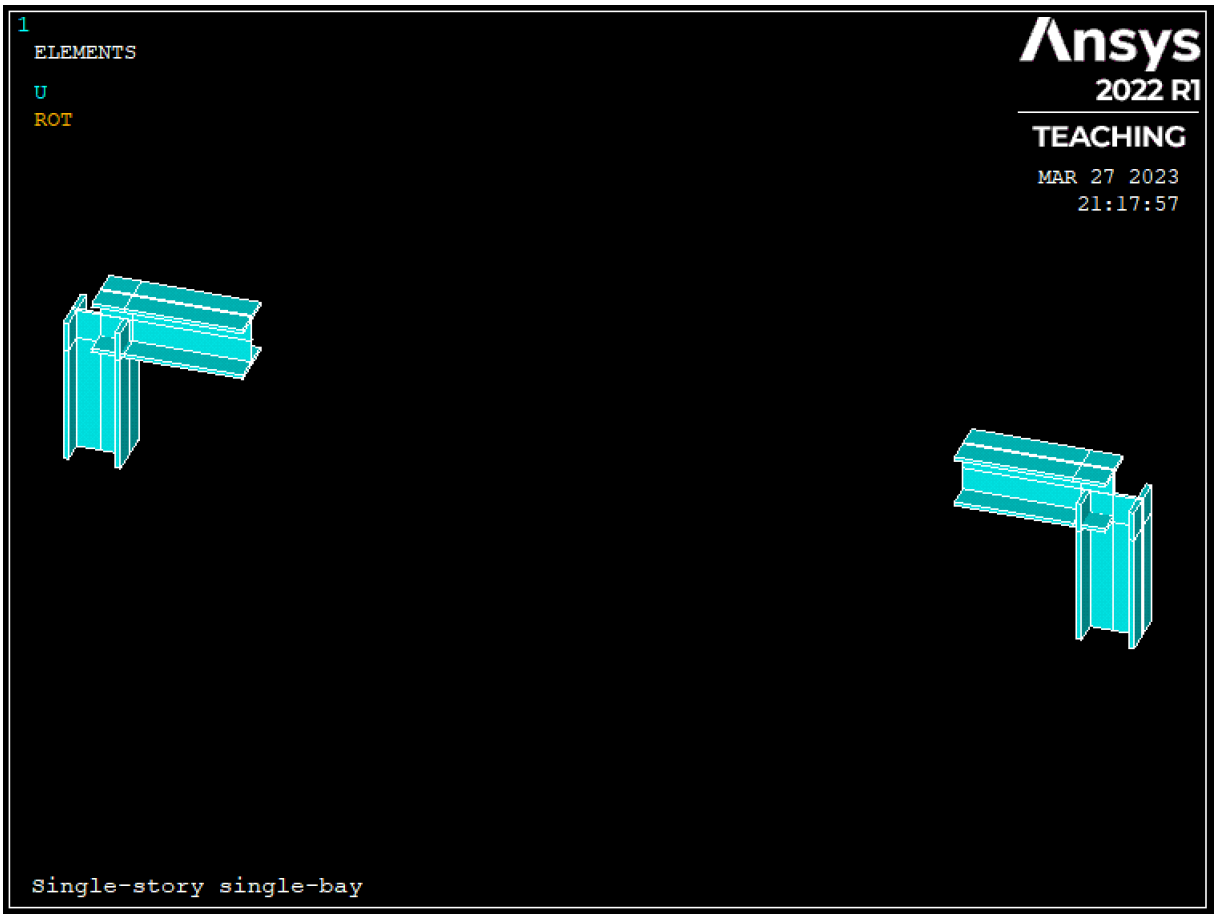

Figure 3.2: Location of Plastic Hinges

The plastic hinges were assigned linear elastoplastic material properties, while the remainder of the steel elements in the frame were assigned elastic perfectly plastic material properties. The Poisson's ratio was chosen according to (Norge, 2005). As in (Dickof, 2013), a yield strength of 350 MPa was increased by a factor of 1,1, resulting in a yield stress of 385 MPa. The post-yield tangent modulus was defined as 1% of the initial modulus of elasticity. A compressive/tensile strength of 470 MPa was chosen for the linear elastoplastic material. The hybrid system reaches its ultimate strength when the plastic hinges achieve this stress. Table 3.4 presents a summary of the material properties of steel.

Table 3.4: Material Properties of Steel

Material	E	ν	f_y	E_p	f_u
Elastic Perfectly Plastic	200 GPa	0,3	385 MPa	-	-
Linear Elastoplastic	200 GPa	0,3	385 MPa	2 GPa	470 MPa

Where:

E	is the modulus of elasticity
v	is Poisson's ratio
f_y	is the yield stress
E_p	is the plastic tangent modulus
f_u	is the compressive/tensile strength

3.3.3. Connection Modeling

As in (Dickof, 2013), the CLT panel was connected to the foundation, and to the steel frame on all sides. Because no foundation is modeled in ANSYS, nodes with restrictions in all degrees of freedom were created just below the corresponding nodes of the panel. These nodes were then used as one of the two required to define a connection.

Two types of springs were used in the model, COMBIN39 and COMBIN40. The COMBIN39-element was used for the axial and shear connections, while the COMBIN40-element was used for contact modeling.

3.3.3.1. COMBIN39

The COMBIN39-element was used for axial and shear connectors. The element has unidirectional capabilities defined by a nonlinear force-deflection curve. Two nodes define the element: one on the steel frame and one on the correlating node of the panel (ANSYS, s.a.-b). Figure 3.3 shows the geometry of COMBIN39.

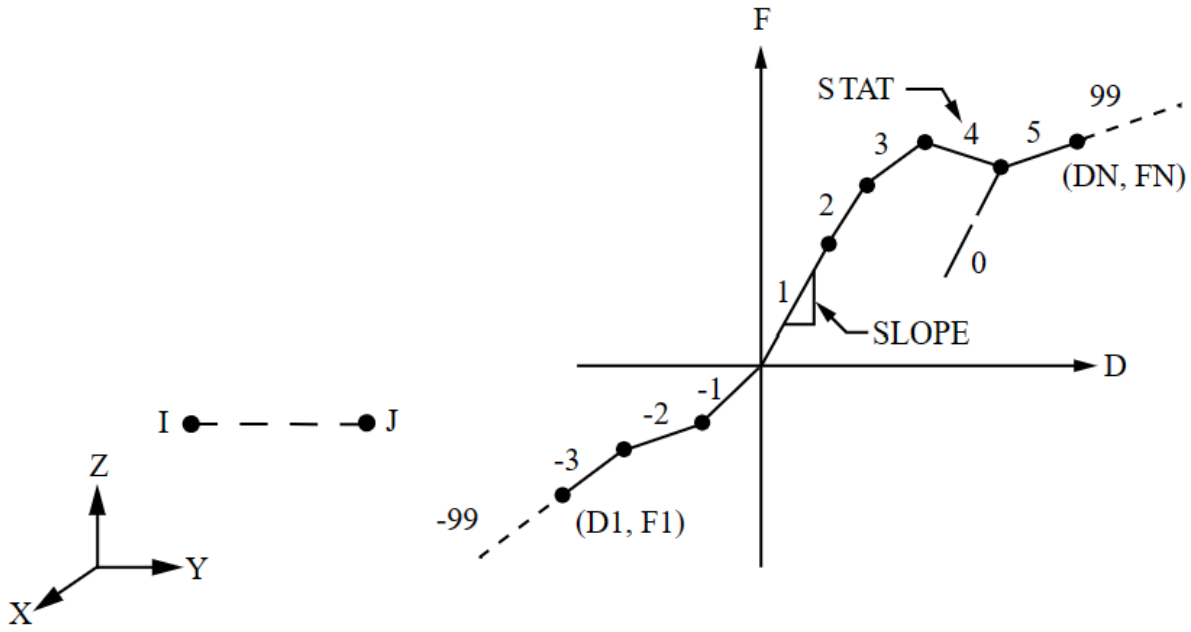

Figure 3.3: COMBIN39 Geometry

Source: ANSYS, I. (s.a.-b). *COMBIN39.* Available at: https://www.mm.bme.hu/~gyebro/files/ans_help_v182/ans_elem/Hlp_E_COMBIN39.html (accessed: 19.04.2023).

The force-deflection points used as input in ANSYS are based on results from the semi-static cyclic test with nailed steel brackets in CLT walls performed by (Schneider, 2009) and the P*inching4* material implementation used in OpenSees by (Dickof, 2013).

Figure 3.4 shows the multilinear force-displacement curve for COMBIN39, while Appendix A presents the associated data points.

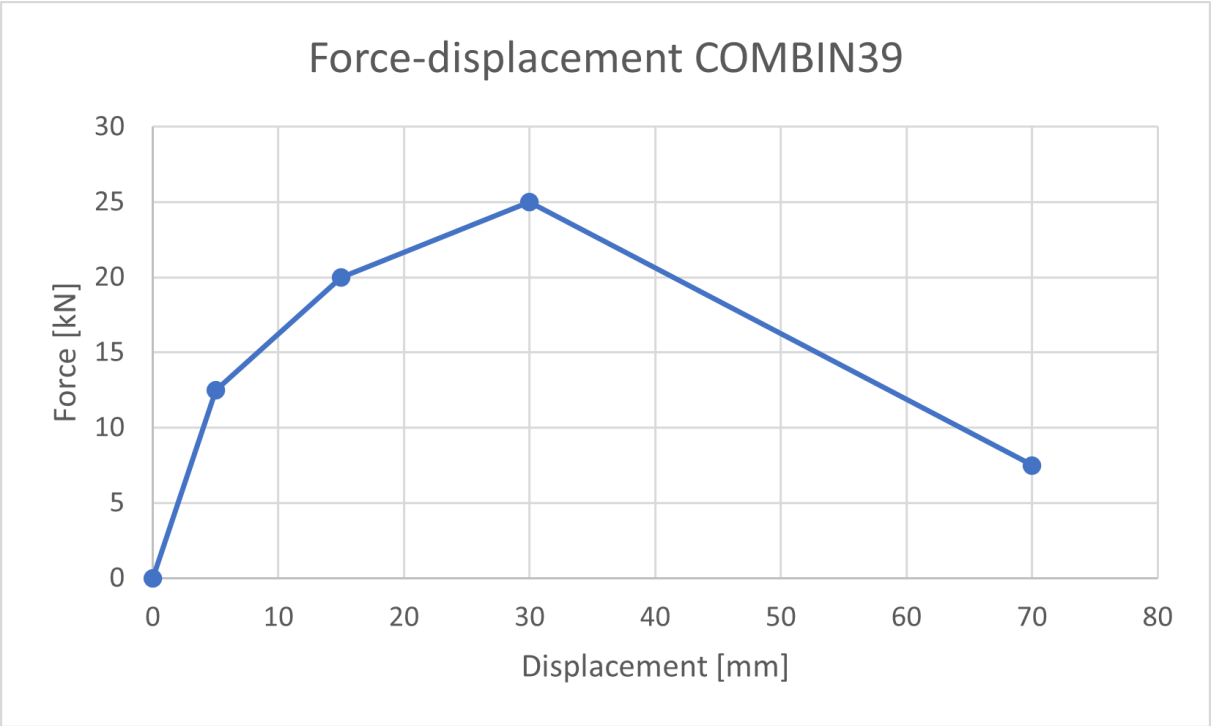

Figure 3.4: Force-Displacement Curve for COMBIN39-Element

3.3.3.2. COMBIN40

The COMBIN40-element was used to model the contact between the steel frame and the CLT panel. The element consists of a spring-slider and damper in parallel, coupled with a gap in series. The spring, slider, damper, and gap properties can be removed (ANSYS, s.a.-c). Only one spring (K2) and the gap property were used for the analysis. Figure 3.5 shows the geometry of COMBIN40.

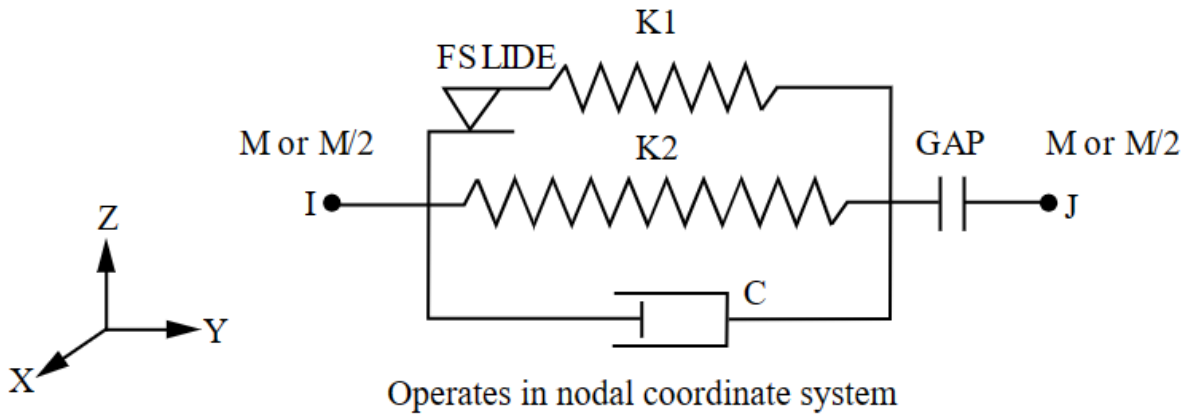

Figure 3.5: COMBIN40 Geometry

Source: ANSYS, I. (s.a.-c). *COMBIN39.* Available at: https://www.mm.bme.hu/~gyebro/files/ans_help_v182/ans_elem/Hlp_E_COMBIN40.html (accessed: 22.04.2023).

COMBIN40 was defined using the same nodes as COMBIN39. An initial gap of 20 mm is assigned to the element. After the gap is closed, ultra-high stiffness kicks in, limiting the movement of the nodes relative to each other. This behavior represents the contact between the two materials, and the hybrid system significantly gains stiffness.

3.4. Loading

In addition to lateral loads, gravity loads affect the system. Table 3.5 lists the dead load from the proposed concrete slab taken as in (Dickof, 2013). The load depth of the frame was 3m.

Table 3.5: Dead Load from Concrete Slab

Dead load slab	Dead load on the beam	Dead load per column
4,05 kPa	12,15 kN/m	36,45 kN

The dead load was applied at the nodes joining the beams and columns. The weight of the steel frame and the CLT panel was neglected.

3.4.1. Static Pushover Loading

A static pushover analysis can be performed by applying a point load on each floor along the structure's height. The loads are then linearly increased, and the horizontal deformation of the

structure is measured at each step. Usually, an even or inverted triangular distribution is used to determine the load magnitude on each floor (Dickof, 2013).

Because the hybrid system is a single-story structure, no load distribution is necessary. The entire lateral load is applied as a point load at the top-left corner of the structure, at the node joining the beam and column together. Figure 3.6 indicates the gravity and lateral load placements using red arrows.

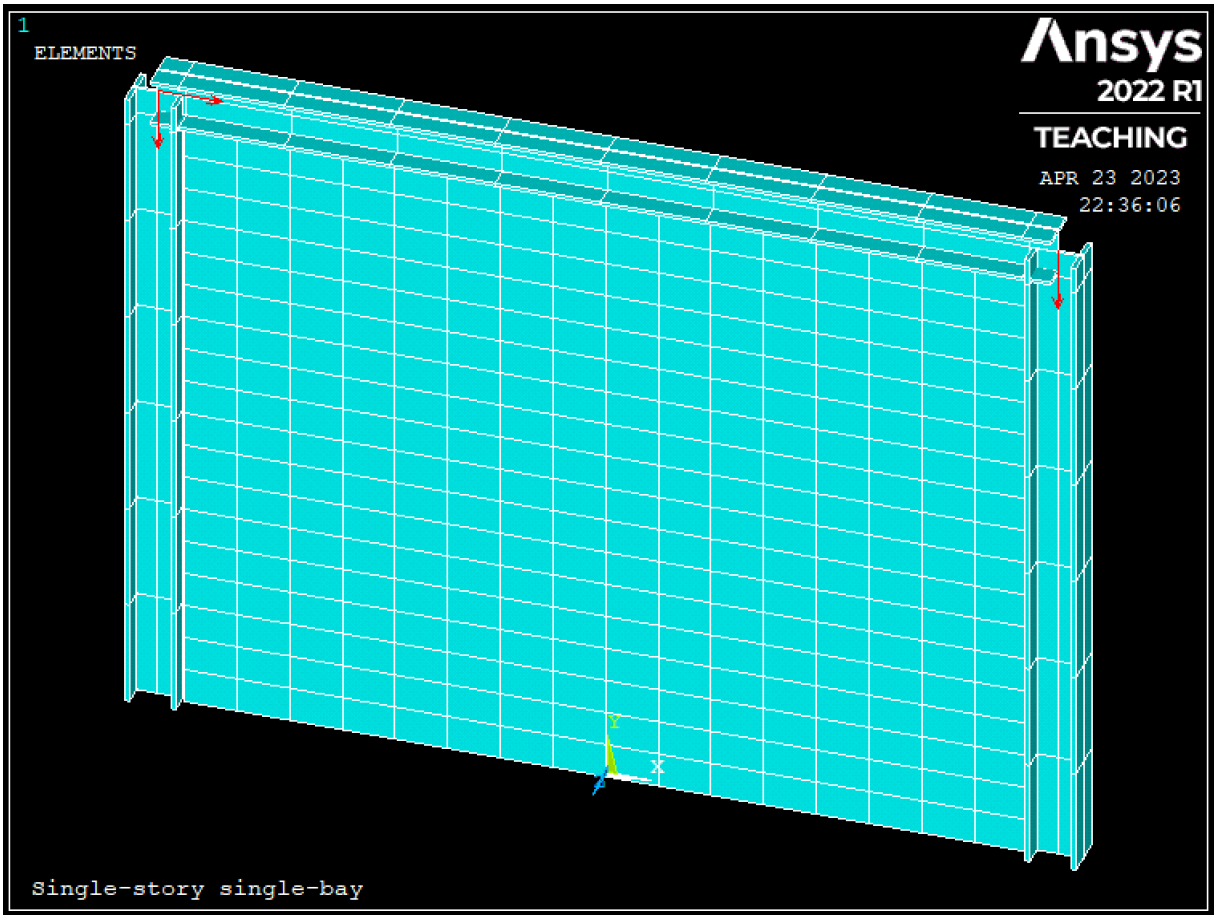

Figure 3.6: Gravity and Lateral Load Placement

The lateral load was applied with equal increments using 15 substeps until it reached a magnitude of 3500 kN. Then, for each substep, the deformation was measured and stored in variables for post-processing using ANSYS's Time-History Postprocessor (ANSYS [Computer software], 2022).

3.5. Parametric Analyses

After the reference model was analyzed, a series of parametric analyses were performed to determine which parameter adjustments achieved a more desirable system performance. The

following four parameter analyses were performed: frame span, connection spacing, perforations in the CLT panel, and CLT panel thickness.

3.5.1. Frame Span

Analyzing the frame span is an interesting parameter to study because it can significantly affect the system's overall performance. The span of a moment-resisting frame with a CLT infill affects the structure's lateral stiffness, strength, and energy dissipation capacity. A wider frame can increase the stiffness and strength of the system but may also increase the weight and cost of the structure. Contrary, a narrower frame may reduce material usage and cost, resulting in a more cost-effective and lightweight structure. Cost and weight analyses are not part of the scope of this study but can be an intriguing topic for future research.

By performing a parametric analysis of the frame span, the optimum span that provides the desired level of performance can be determined. The analysis can help understand the trade-offs between different design parameters and select the most appropriate configuration for a specific project's requirements. Through optimizing the design, structures can become more robust and reliable, with a decreased risk of failure.

The height of the hybrid system remained constant during the parametric analysis. Table 3.6 presents the frame span configurations and the corresponding number of connectors employed.

Table 3.6: Frame Spans and Corresponding Connectors for Parametric Analysis

Configuration	Reference model	Case 1	Case 2	Case 3
Span	6 m	7 m	8 m	9 m
Connectors along the width	9	10	11	12

3.5.2. Connection Spacing

The connection spacing refers to the maximum distance between the connectors that connect the CLT panel to the steel frame. As the connection spacing increases, fewer connectors are used, and the system's stiffness decreases. In contrast, reducing the connection spacing increases the number of connectors, resulting in a stiffer system.

By performing a parametric analysis of the connection spacing, the relationship between the number of connectors used and the stiffness of the system can be identified. The analysis can help make informed decisions regarding connection design to optimize the hybrid system performance.

In addition to the maximum connection spacing of the reference model, Table 3.7. presents the considered connection spacing configurations.

Table 3.7: Connection Spacings for Parametric Analysis

Configuration	Case 1	Reference model	Case 2	Case 3
Maximum connection spacing	700 mm	800 mm	900 mm	1000 mm
Connectors along the width	10	9	8	7
Connectors along the height	8	7	6	6

3.5.3. Perforations in CLT Panel

Perforations in CLT panels are necessary for shear walls with doors and windows. Analyzing the effect of perforations in the CLT panel is an important parameter to consider because it can provide valuable insights into how openings affect the overall performance of the hybrid system. Perforations alter the stress distribution within the CLT panel and can lead to stress concentrations around the opening edges. By introducing different amounts, sizes, and shapes of perforations, we can determine how these changes affect the structural behavior of the system, including its stiffness and strength.

Two cases are investigated in this study. In the first case, a single perforation was centered with respect to the width of the panel, stretching from the foundation to 2,1 m up. This perforation was made to fit a door. For the second case, two perforations were placed along the width of the panel, each 1,5m from the outer edges. The perforations were centered with respect to the height of the panel. These perforations were made to fit two tall and narrow windows. Table 3.8 presents the considered perforation configurations.

Table 3.8: Perforations for Parametric Analysis

Configuration	Case 1	Case 2
Perforation Type	Door	Window
Width x Height	1000 x 2100 mm	2 x (750 x 2500 mm)
Total Perforation Area	2,1 m^2	3,75 m^2

Figure 3.7 and Figure 3.8 shows the placement of the door and window perforations, respectively.

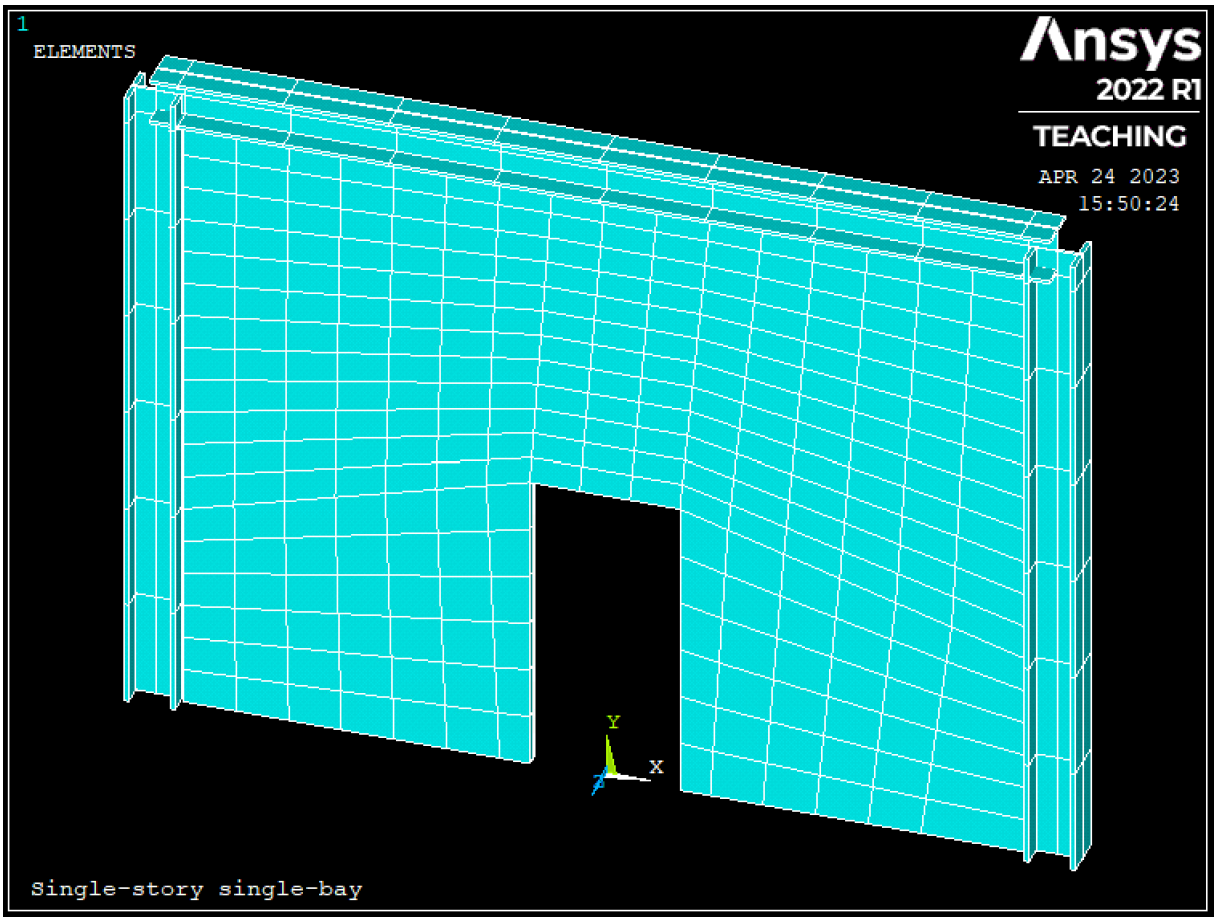

Figure 3.7: Placement of Door Perforation

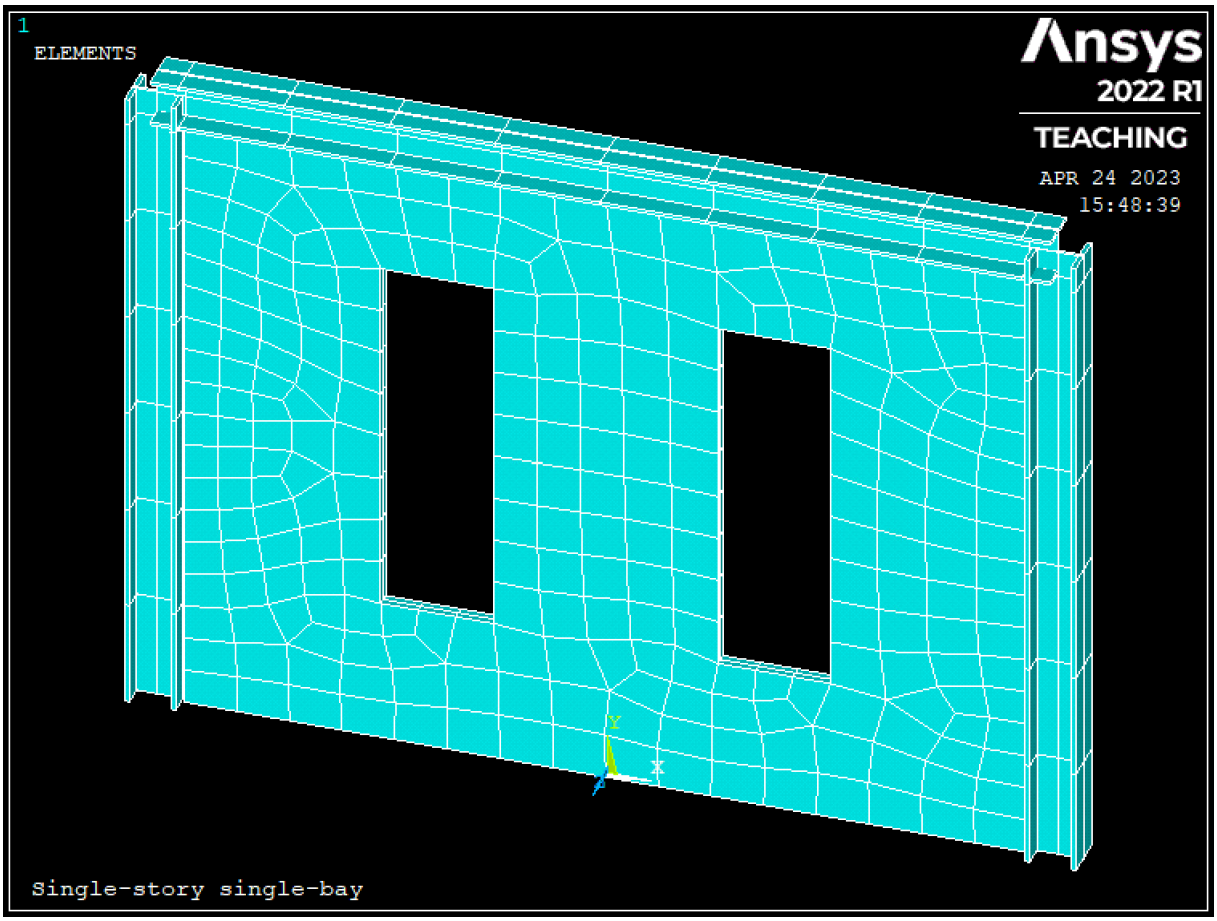

Figure 3.8: Placement of Window Perforations

3.5.4. CLT Panel Thickness

The thickness of the CLT panel is an important parameter to analyze because it directly affects the stiffness and strength of the infill system. Therefore, by varying the thickness of the CLT panel, we can investigate the effects of panel stiffness on the overall performance of the hybrid system.

Increasing the thickness of the CLT panel leads to higher stiffness and strength, resulting in better performance when subjected to lateral loads. However, increasing the thickness of the panel also leads to an increase in weight and cost, which can be significant limiting factors. Therefore, by analyzing the effect of the thickness of the CLT panel, informed decisions on the appropriate thickness required to meet the desired performance and functional requirements can be made.

In addition to the 99mm thickness of the CLT panel in the reference model, five panels, commercially available from Stora Enso, were analyzed. Table 3.9 presents the panel properties, which can also be found at (Enso, s.a.).

Table 3.9: CLT Panel Properties for Parametric Analysis

Configuration	Case 1	Reference model	Case 2	Case 3	Case 4	Case 5
Thickness [mm]	80	99	120	140	160	180
Type	C3s	C3s	C5s	C5s	L5s	L5s
Layers	20-40-20	33-33-33	30-20-20-20-30	40-20-20-20-40	40-20-40-20-40	40-30-40-30-40

Source: Enso, S. (s.a.). *Cross-laminated timber (CLT).* Available at: https://www.storaenso.com/en/products/mass-timber-construction/building-products/clt (accessed: 24.04.2023).

4. Results

This section presents the results of the investigation into the use of CLT-steel hybrid shear walls as seismic force-resisting systems. The results are exported as force-deformation data from the Time-History Postprocessor (ANSYS [Computer software], 2022). The horizontal deformation is then divided by the initial frame span to present the horizontal deformation results in percent (mm/mm). A scatter chart with straight lines and markers is used to plot the results, with a black cross indicating the ultimate strength of the configurations.

First, the results of the reference model analysis are presented, followed by the parametric analysis results, including the effects of varying frame span, connection spacing, perforations, and panel thickness.

The von Mises stress distribution in the steel frame and CLT panel for the reference model is shown in this section. In addition, the von Mises stress distribution in the CLT panel is shown for both perforation configurations considered in the parametric analyses. Finally, Appendix C shows the von Mises stress distribution in the CLT panel for the remaining parametric analysis configurations.

4.1. Reference Model

Figure 4.1 shows the horizontal deformation of the reference model. The deformation is compared to a bare steel frame with equivalent geometric and material properties.

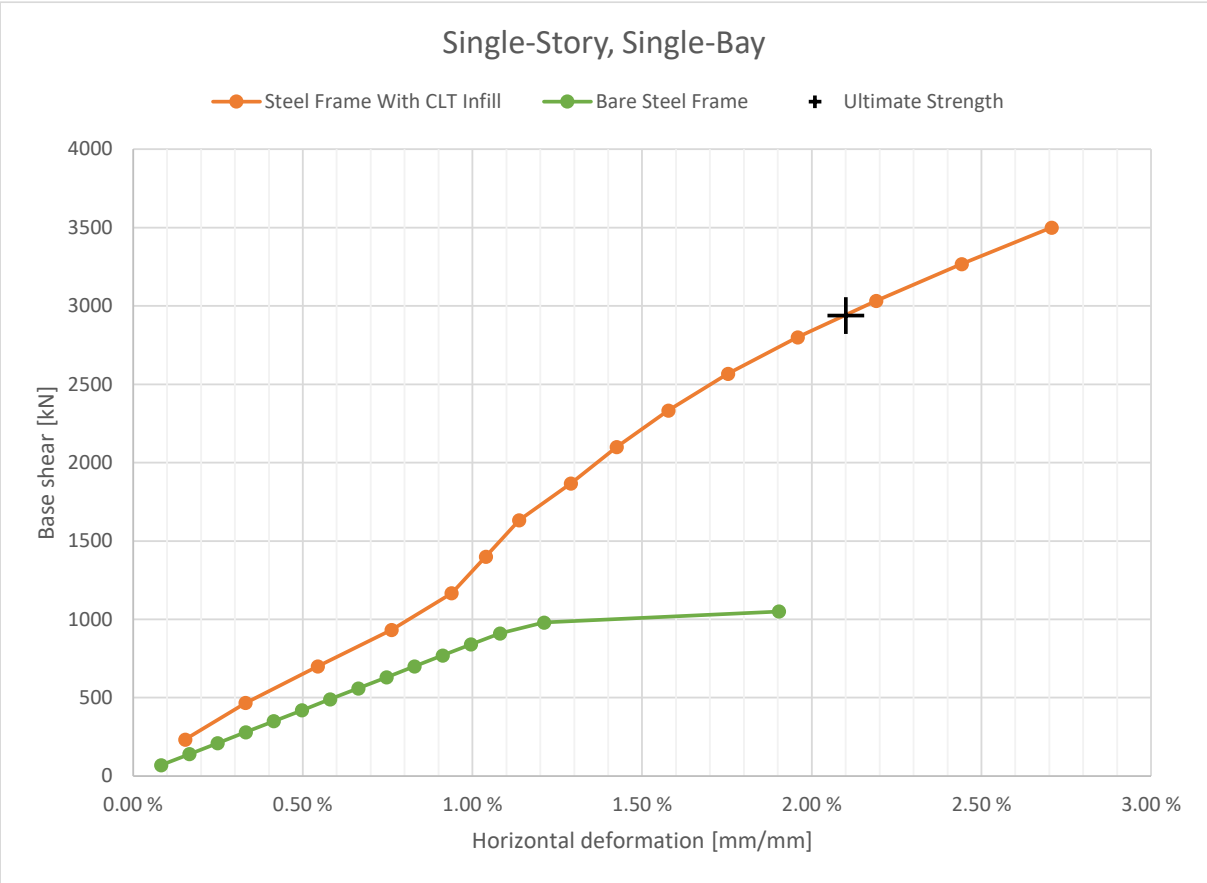

Figure 4.1: Results for the Reference Model

The stiffness of the steel frame with CLT infill appears almost linear until it approaches a value just below 1% horizontal deformation. At this point, a sudden increase in stiffness occurs. After that, the stiffness steadily decreases until a horizontal deformation of 2,1%, where the base shear is 2940 kN, and the system reaches its ultimate strength.

The bare steel frame deforms linearly until reaching 1,1% deformation, where it yields and subsequently loses next to all its stiffness. The yielding occurs at a base shear of 1000 kN.

Figure 4.2 and Figure 4.3 show the von Mises stress distribution at ultimate strength in the steel frame and CLT panel, respectively.

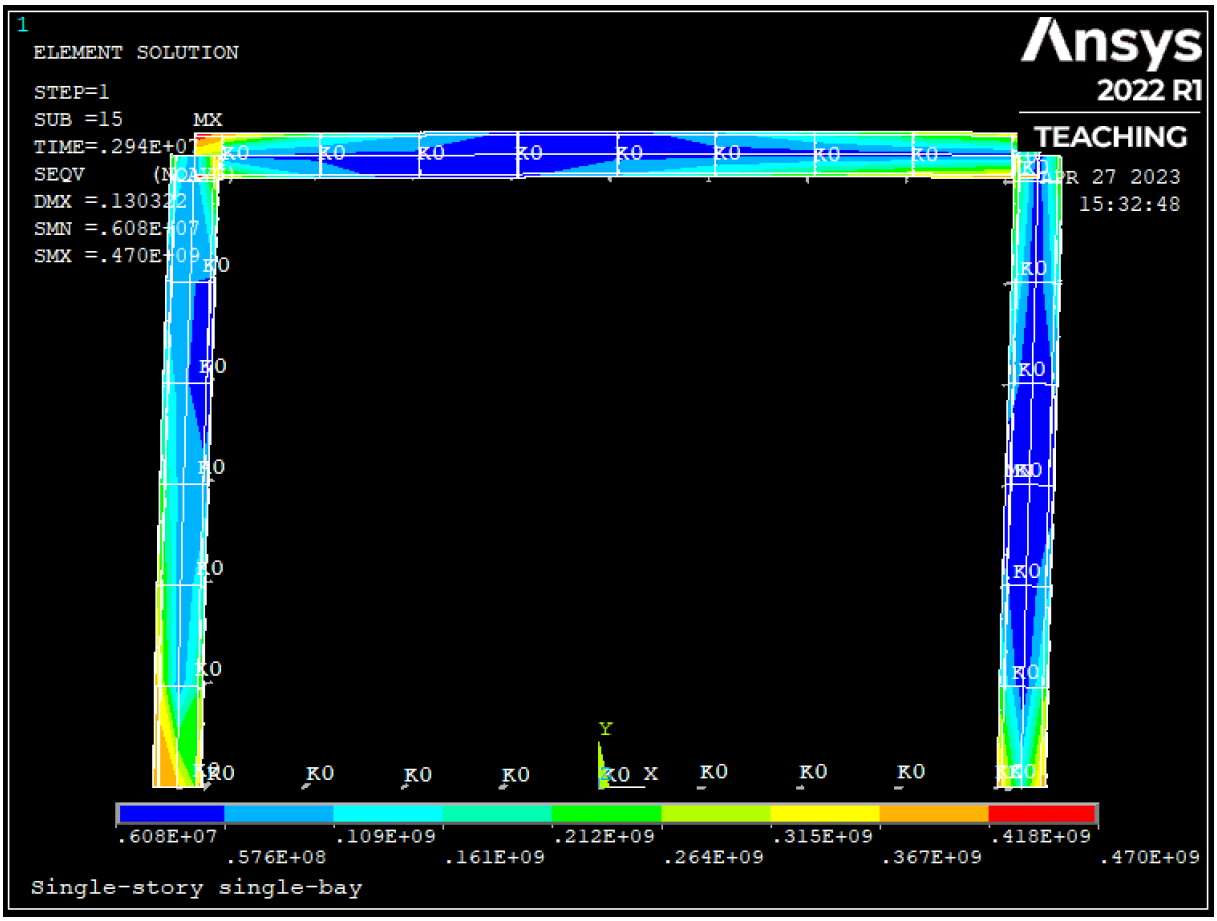

Figure 4.2: Von Mises Stress Distribution in Steel Frame – Reference Model

The von Mises stress is maximum at and around the beam-to-column and column-to-foundation connections. There is a steady decrease in stress towards the middle of the frame members. The linear elastoplastic steel reaches its ultimate stress when the base shear rises to 2940 kN, as defined in Table 3.4. The fracture occurs at the top left corner of the frame, around the beam-to-column intersection point.

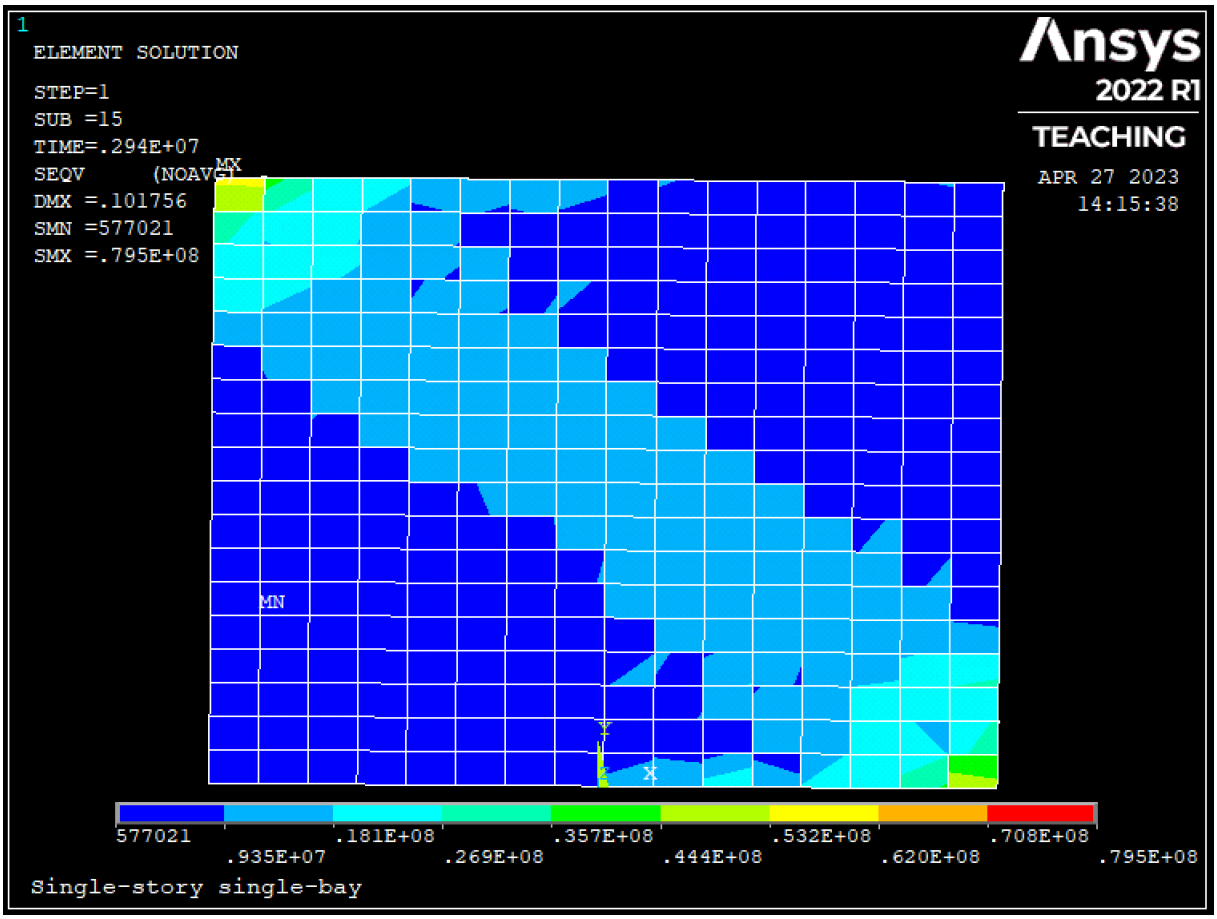

Figure 4.3: Von Mises Stress Distribution in CLT Panel – Reference Model

The CLT panel acts as a compression strut, with the maximum von Mises stresses occurring along the diagonal axis of the panel. Consequently, high stress concentrations are registered at two contact points between the steel frame and the CLT panel: the top left (where the load is applied) and the bottom right (opposite corner, where the panel is pushed against the restricted column).

4.2. Parametric Analyses

For simple identification, R.M., for reference model, and the case number of each configuration is parenthesized in the legend of the plots.

4.2.1. Frame Span

Figure 4.4 shows the horizontal deformation for all frame spans considered in the parametric analysis.

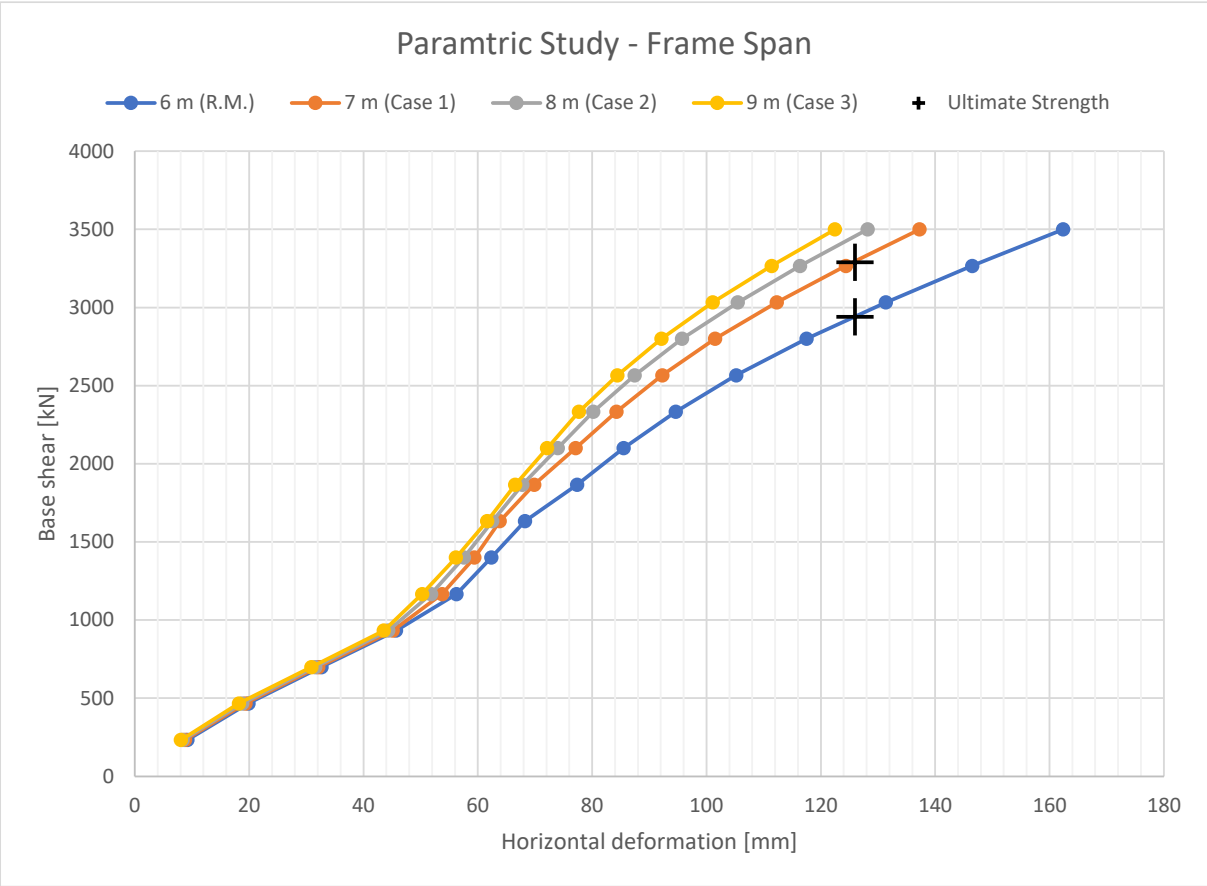

Figure 4.4: Results of Parametric Study – Frame Span

For the frame span parametric analysis, the horizontal deformation is not divided by the initial span, instead being left as exported from ANSYS (ANSYS [Computer software], 2022).

The behavior of the configurations is roughly the same until the system reaches a 45 mm horizontal deformation. At this point, the stiffnesses of the different configurations begin to increase considerably. For the larger spans, the stiffness increase is more considerable and occurs at slightly lesser loads. Then, as in the reference model, the stiffnesses steadily decrease until the configurations reach their ultimate strength.

For case 1, the steel fractures at a base shear of 3290 kN when the configuration reaches a 126 mm horizontal deformation. The larger frame spans do not experience steel fracture within a load magnitude of 3500 kN.

4.2.2. Connection Spacing

Figure 4.5 shows the horizontal deformation for all connection spacings considered in the parametric analysis.

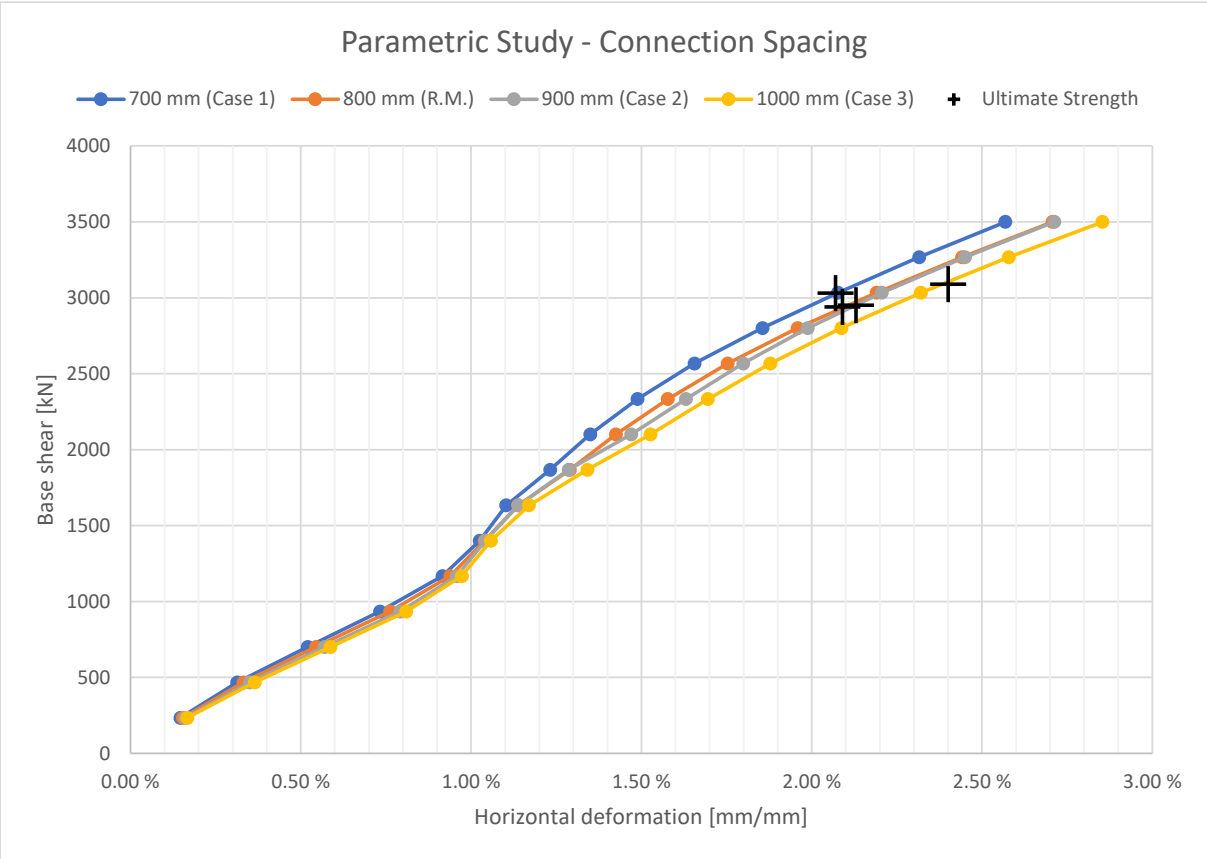

Figure 4.5: Results of Parametric Study – Connection Spacing

Small-scale differences in stiffness are observable before the system reaches 1% horizontal deformation. At this point, the stiffness of all the configurations increases before decreasing at about 1,1% deformation. The fact that the stiffnesses fall at different rates makes the effect of the connection spacing evident.

All configurations reach their ultimate strength at base shears of roughly 3000 kN, except case 3, which differs slightly with a 3090 kN base shear capacity.

4.2.3. Perforations in CLT Panel

Figure 4.6 shows the horizontal deformation for both the perforation configurations considered in the parametric analysis.

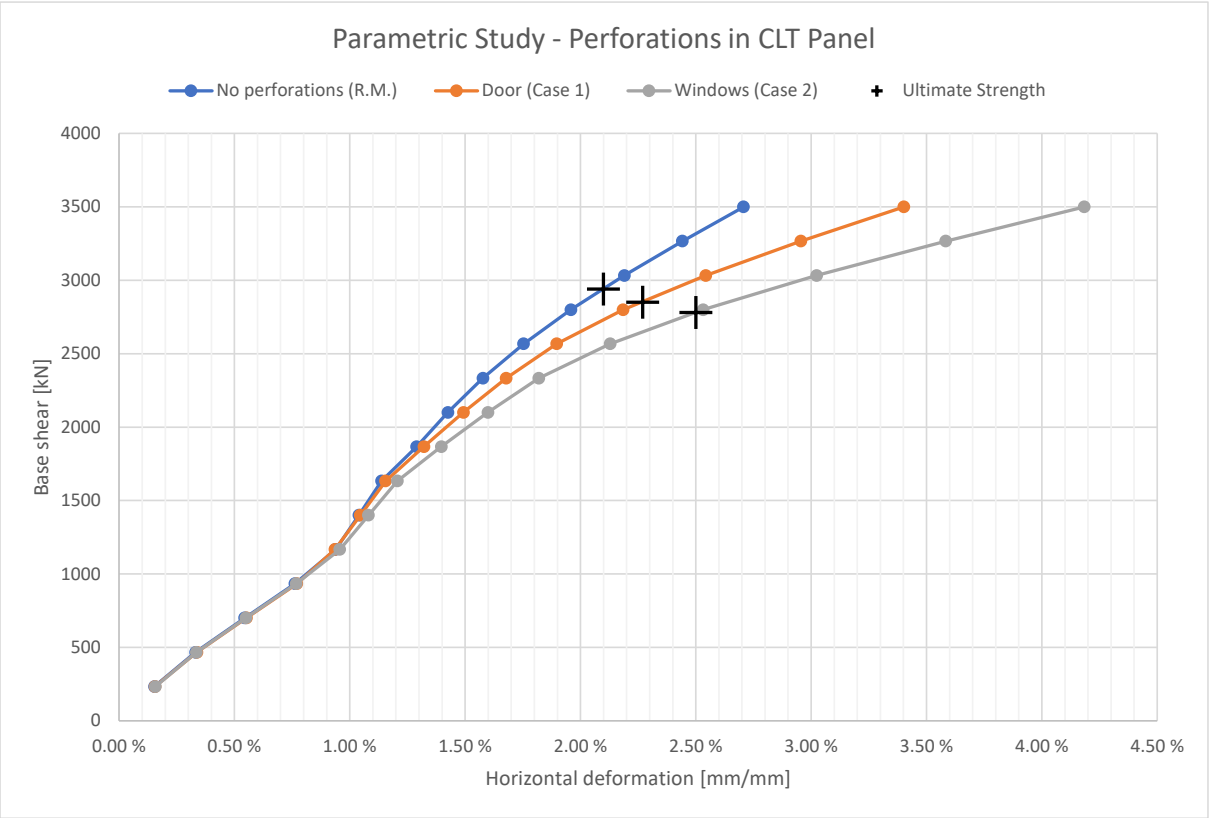

Figure 4.6: Results of Parametric Study – Perforations in CLT Panel

The effect of the perforations is first observable just before the system reaches 1% horizontal deformation. After that, the perforations substantially affect the horizontal deformation of the hybrid system. The deformation increases, and the configurations reach their ultimate strength at lesser base shears for more extensive perforations.

At base shears of 2780 kN and 2850 kN, steel fracture occurs when window and door perforations are implemented, respectively.

Figure 4.7 and Figure 4.8 show the von Mises stress distribution at ultimate strength in the CLT panel for the door and window perforations, respectively.

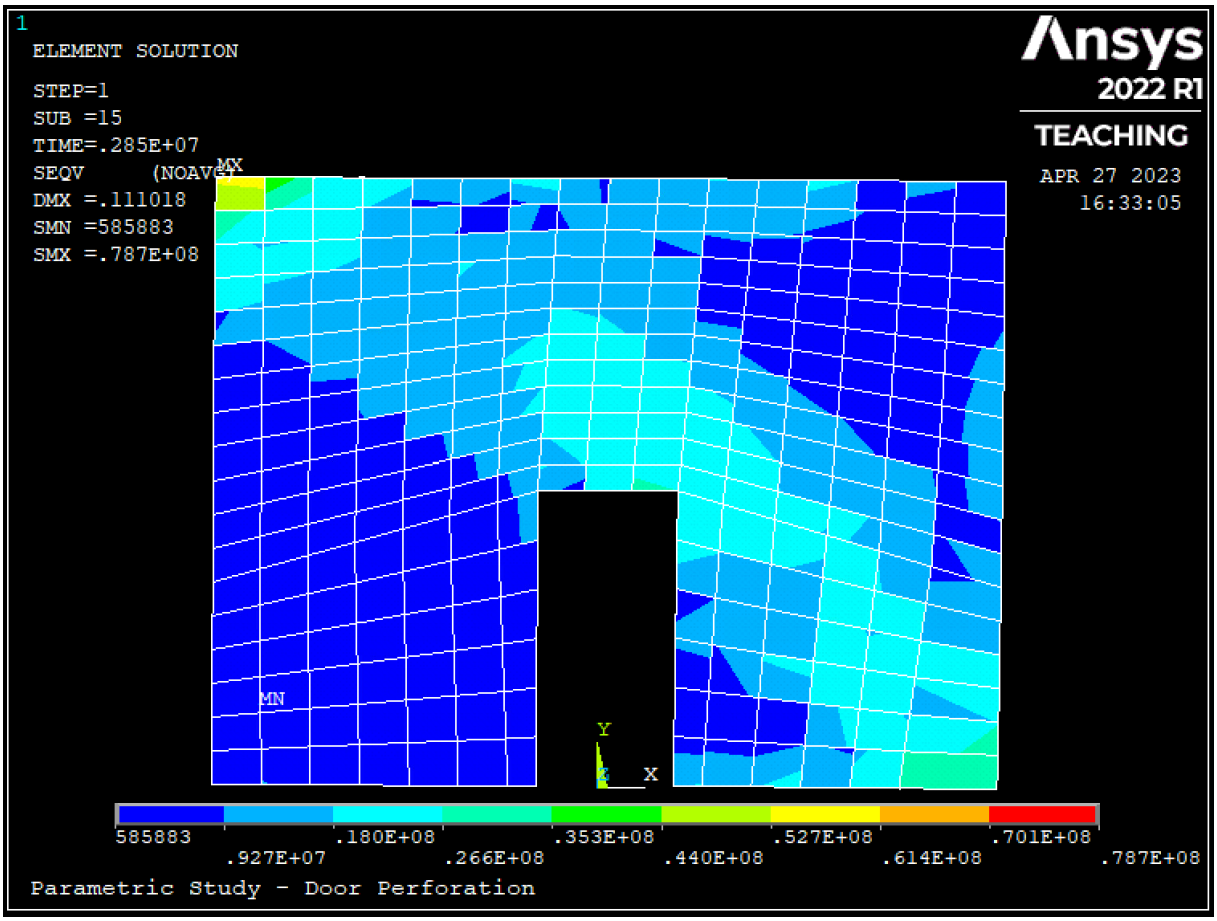

Figure 4.7: Von Mises Stress Distribution in CLT Panel – Door Perforation

The door perforation alters the stress distribution in the CLT panel compared to Figure 4.3 of the reference model. The CLT panel still acts as a compression strut, but the stress path is slightly curved. Instead of following the diagonal of the panel, it bends around the top right corner of the perforation, where high stress concentrations occur. In addition, high stress concentrations form at both ends of the diagonal.

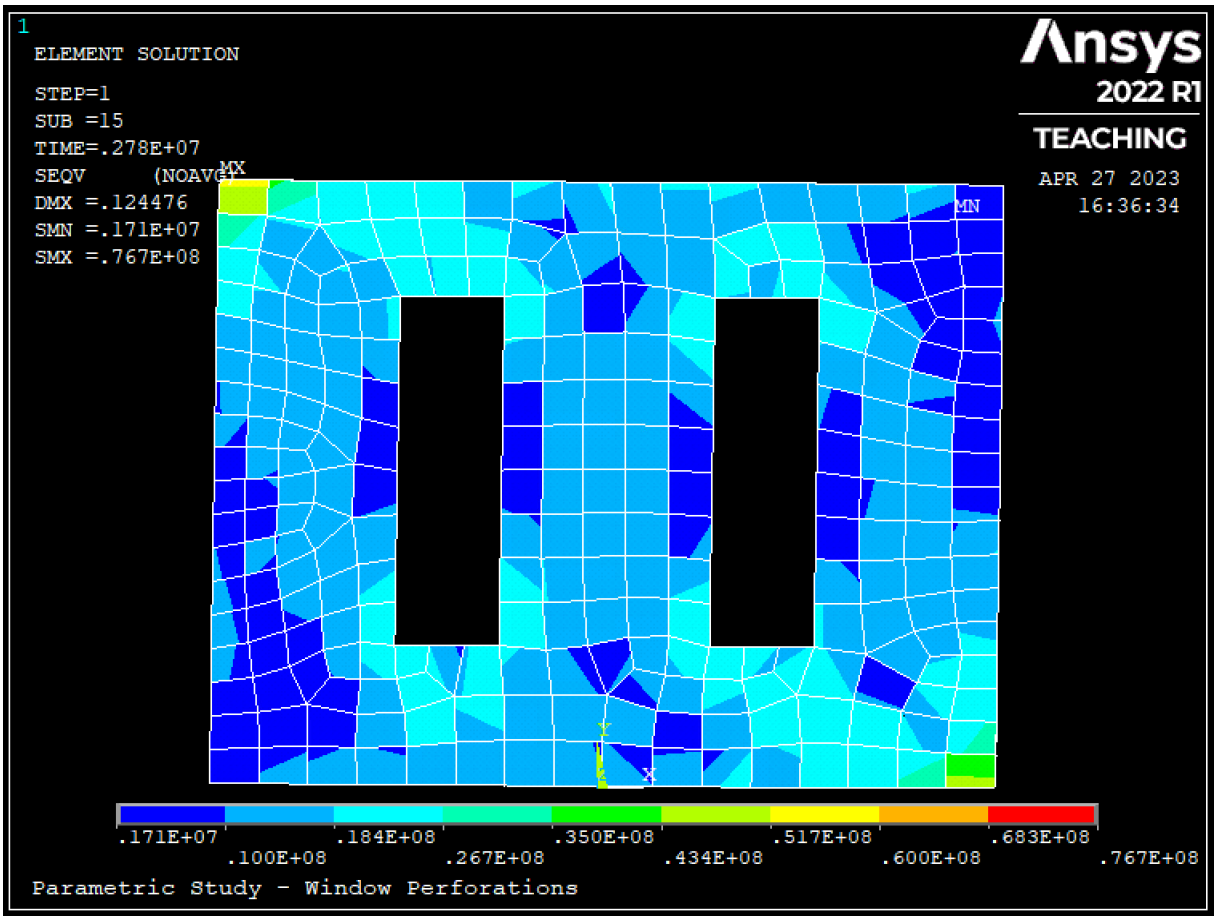

Figure 4.8: Von Mises Stress Distribution in CLT Panel – Window Perforations

The window perforations alter the stress distribution even more than the door perforation. A stress path along the diagonal is no longer possible, as the perforations are in the way. Instead, the von Mises stresses are more evenly distributed across the whole panel. As a result, high stress concentrations form at the perforation corners and opposite ends of the panel (top left and bottom right).

4.2.4. CLT Panel Thickness

Figure 4.9 shows the horizontal deformation for all the CLT panel thicknesses considered in the parametric analysis.

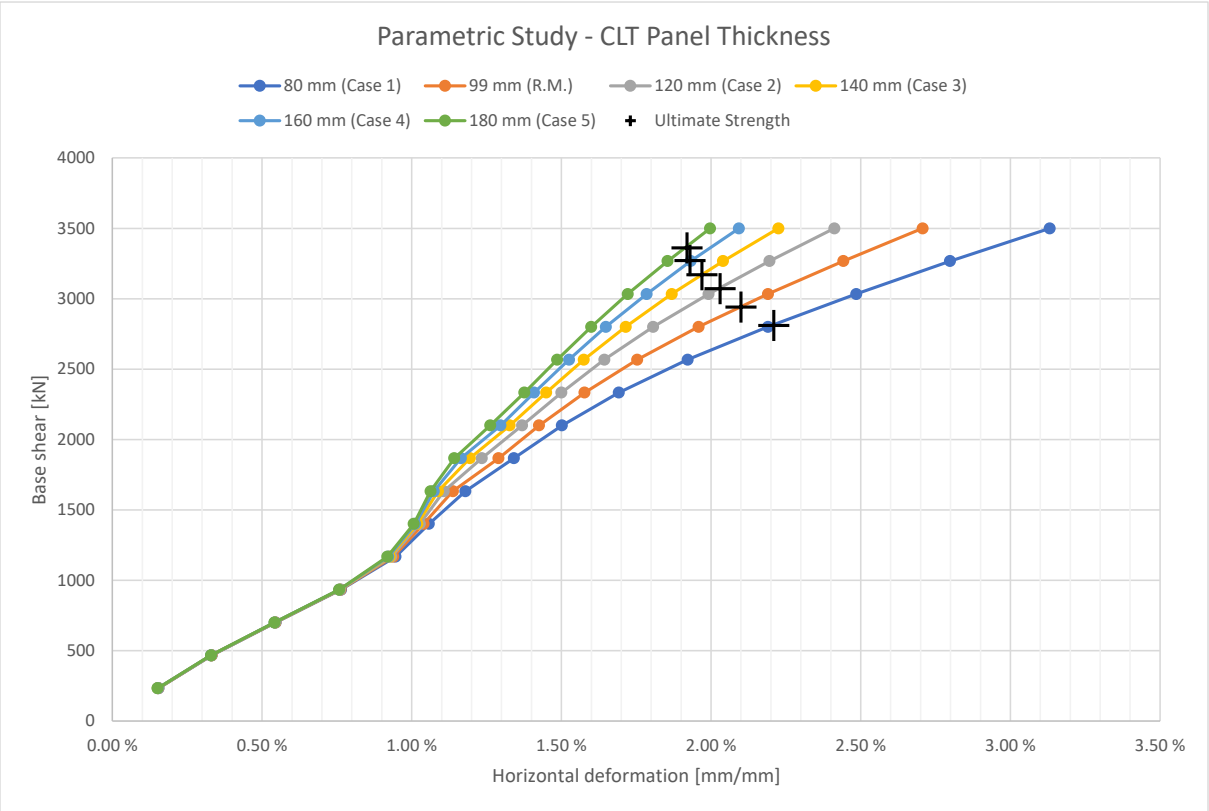

Figure 4.9: Results of Parametric Study – CLT Panel Thickness

As in the parametric analysis on perforations in the CLT panel, the effect of the thickness of the panel is first observable just before the system reaches 1% horizontal deformation. At this point, the configurations begin to differ. The thicker CLT panels have a more rapid increase and, subsequently, a slower decrease in stiffness. The difference in horizontal deformation at equivalent base shears becomes progressively evident as the load increases.

As the thickness of the panel increases, higher base shears are needed for the linear elastoplastic steel to reach its ultimate stress. As a result, the thinnest and thickest panel configurations reach their ultimate strength at base shears of 2810 kN and 3360 kN, respectively.

5. Discussion

This section discusses the results obtained from the investigation into using CLT-steel hybrid shear walls as seismic force-resisting systems. In addition, the section presents the limitations of the study and a comparison with the results from (Dickof, 2013). The discussion of the obtained results is intended to provide a comprehensive understanding of the performance of CLT-steel hybrid shear walls and to identify areas for future research.

5.1. Limitations

5.1.1. Yield Criterion

The model in (Dickof, 2013) yields when it reaches a defined yield moment, whereas ANSYS Mechanical APDL only allows for principal stress as the yield criterion. There are benefits to using the moment-curvature relationship as a yield criterion. As the cross-section is assumed to remain plane during yielding, the entire cross-section yields simultaneously, instead of local yielding at outer parts of the cross-section experiencing high stresses. Additionally, and specifically for moment-resisting frames, it allows for the consideration of the strength and behavior of the frame as a system rather than individual members. This is because a member's curvature depends on that of the adjacent members. Using the yielding moment as the yield criterion can result in a more effective design.

5.1.2. Stress Concentrations and Mesh Size

As presented in Section 3.3.3, two nodes define the connectors and the contact modeling. The node on the CLT panel is centered with respect to the thickness of the panel (z-coordinate = 0). When the connectors act in tension or compression, the panel is pulled or pushed at the node, resulting in a local deformation. This effect is even more apparent when contact between the steel frame and the CLT panel occurs. The COMBIN40-element was implemented to model node-to-node contact. When the gap of 20 mm is closed, the node on the CLT panel experiences substantial stress. As the node on the panel absorbs forces, it deforms inwards (towards the

interior of the panel). Figure 5.1 shows the local deformation at the top left corner of the panel at ultimate strength for the reference model.

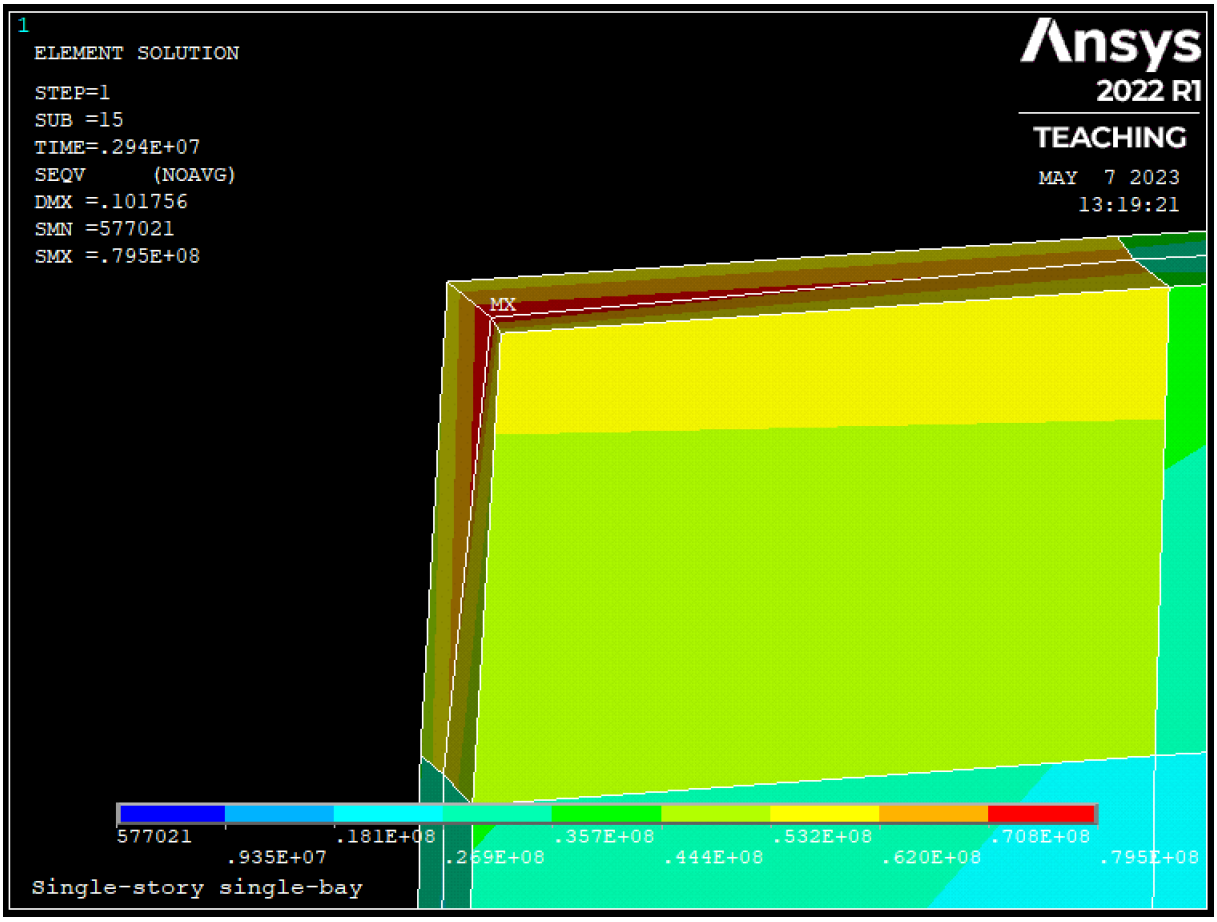

Figure 5.1: Local Deformation at Top-Left Corner of CLT Panel

When a structure experiences a significant variation in stress within a small and confined region, the stress is referred to as stress concentration. A point or line contact area is exceedingly small, resulting in high stresses even under small loads. Contact stresses demonstrate high stress gradients that recede quickly, moving away from the region (Young et al., 2012). They quickly recede because the contact region carries a significant portion of the load, relieving the adjacent regions of stress.

The stress concentrations increase with a more refined mesh on the CLT panel because the contact stresses are distributed on smaller mesh elements. Therefore, using a more refined mesh increases stress concentrations, resulting in a more extensive local deformation at the contact node. Contrarily, the stress concentrations are reduced by utilizing a less refined mesh. As a result, parametric analyses that involve changing the mesh size may lead to results that are not entirely comparable to those obtained from the reference model.

The correlation between the mesh size of the CLT panel and connection spacing can be expressed as follows: two mesh elements are formed per connection spacing along the panel's width, while three mesh elements are formed per connection spacing along its height. A mesh element refers to the interconnected squares created by meshing a solid panel. Therefore, modifying the connection spacings also changes the mesh size. This is particularly relevant in the connection spacing parametric analysis, where the system's geometry remains constant while the mesh size changes for each configuration.

5.2. Reference Model

Reviewing Figure 4.1, the effect of adding a CLT panel to a bare frame is evident. The initial difference in stiffness (until approaching a value just below 1% horizontal deformation) is due to the axial and shear connectors. The COMBIN39-element adds considerable stiffness to the system. Figure 3.4 shows that the element reaches its peak stiffness at 30 mm displacement. The most significant difference in stiffness in the early phases occurs between 0,5% and 1% (30 to 60 mm) horizontal deformation. At 0,5% deformation, the axial and shear connectors closest to the load application point will reach their peak stiffness. As the base shear increases, others nearby follow, and the connection elements altogether achieve their peak stiffness slightly below 1% horizontal deformation. At this point, the steel frame with the CLT infill can withstand 71% more base shear (1200 kN compared to 700 kN) than the bare steel frame to achieve the same deformation.

From here onwards, the two configurations have drastically different behaviors. The bare steel frame continues linearly deforming until it reaches 1,1% horizontal deformation, where it yields and subsequently loses nearly all its stiffness. Finally, at slightly above 1000 kN, it experiences large deformation and fractures.

On the other hand, the steel frame with CLT infill has a significant increase in stiffness slightly below 1% horizontal deformation. This increase in stiffness is a direct consequence of contact between the steel frame and the CLT panel. Once the materials make contact, the panel's stiffness, which is substantially higher than the connections, kicks in. As the panel begins to crush, it loses a substantial amount of stiffness, as presented in Table 3.3. This drop is apparent from 1,2% horizontal deformation onwards. The curve continues to fall until the hybrid system reaches its ultimate strength at 2940 kN base shear and 2,1% horizontal deformation.

Overall, adding a CLT infill to a steel frame raises the base shear needed to reach the ultimate strength of the system by 194%, from 1000 kN to 2940 kN.

The von Mises stress distribution shown in Figure 4.2 and Figure 4.3 reveal reasonably expected results. For the steel frame, high stresses are expected close to the load application point and at the column-to-foundation connections. The CLT panel experiences high stresses along the diagonal from the load application point to the opposite corner. The stresses peak at both ends of the diagonal since contact first occurs in these parts of the hybrid system. In addition, the panel is pushed up and down against the beam and foundation, respectively. Consequently, stresses develop along the upper and lower edges of the panel.

5.3. Comparison With Model in (Dickof, 2013)

Figure 5.2 compares the reference model to the model in (Dickof, 2013).

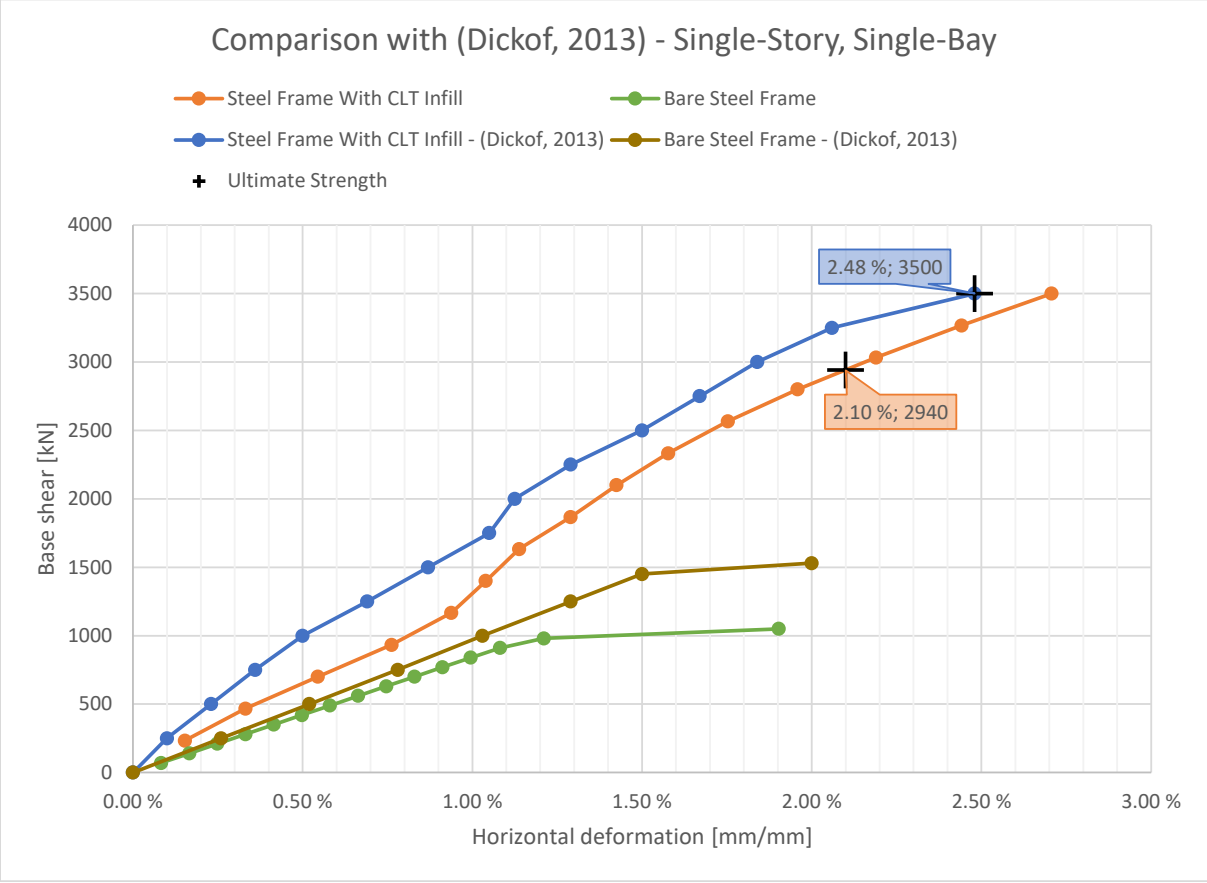

Figure 5.2: Comparison Between the Reference Model and the Model in (Dickof, 2013)

Investigating the bare steel frames, it is evident that the curves display significant similarities. However, the bare steel frame in the reference model is slightly less stiff and yields at less base

shear. The difference in yield strength is considerable, but it can be attributed to the limitation discussed in Section 5.1.1. Further clarifications are provided in Section 5.3.1.

Comparing the steel frames with CLT infill, it is evident that the dissimilarity is more substantial. It is noted that contact between the steel frame and CLT panel appears to occur slightly below 1% horizontal deformation for both models. The model in (Dickof, 2013) is stiffer than the reference model and yields less deformation for all base shear magnitudes. Table 5.1 shows the difference in horizontal deformation for selected base shear magnitudes.

Table 5.1: Difference in Horizontal Deformation for Reference Model and Model in (Dickof, 2013)

Base shear	Deformation for reference model	Deformation for model in (Dickof, 2013)	Difference in deformation
500 kN	0,35%	0,23%	0,12%
1000 kN	0,81%	0,5%	0,31%
1500 kN	1,08%	0,87%	0,21%
2000 kN	1,37%	1,13%	0,24%
2500 kN	1,7%	1,5%	0,2%

As discussed in Section 5.2, the first connectors reach their peak stiffness at 0,5% horizontal deformation. After this point, the difference in deformation between the two models remains relatively constant. The average difference in deformation (for base shears of 1000 kN and above) is 0,24%.

The steel frame and connectors are the main contributors to the stiffness of the system prior to contact between the steel frame and CLT panel. Considering the slight variation in stiffness between the bare steel frame models, it is reasonable to assume that the dissimilarity before contact between the materials can be primarily attributed to the connection design (COMBIN39-element). After contact, the steel frame modeling mainly contributes to the dissimilarity. As with the bare steel frames, the difference in horizontal deformation can be attributed to the limitation discussed in Section 5.1.1. Further clarifications are provided in Section 5.3.1.

The ultimate strength of the hybrid systems also differs. To demonstrate, the model in (Dickof, 2013) reaches its ultimate strength at a base shear of 3500 kN, an increase of 19% compared to the reference model. It is important to note that all of the differences discussed above are on the

conservative side, accounting for the limitations of the analytical models and ensuring safe design.

5.3.1. Modified Yield Stress

Considering that the model in (Dickof, 2013) uses a yield moment as the yield criterion, the reference model can be adjusted to provide a more comparable result. As Figure 5.2 shows, the bare steel frame in the reference model yields at less horizontal deformation than the model in (Dickof, 2013). A modified yield stress that ensures yielding occurs at almost identical base shears for both models can be found by trial and error. As a result, the reference model is modified by increasing the yield stress to

$$f_{y.mod} = 550\ MPa$$

Figure 5.3 compares the reference model and the model in (Dickof, 2013) with the modified yield stress.

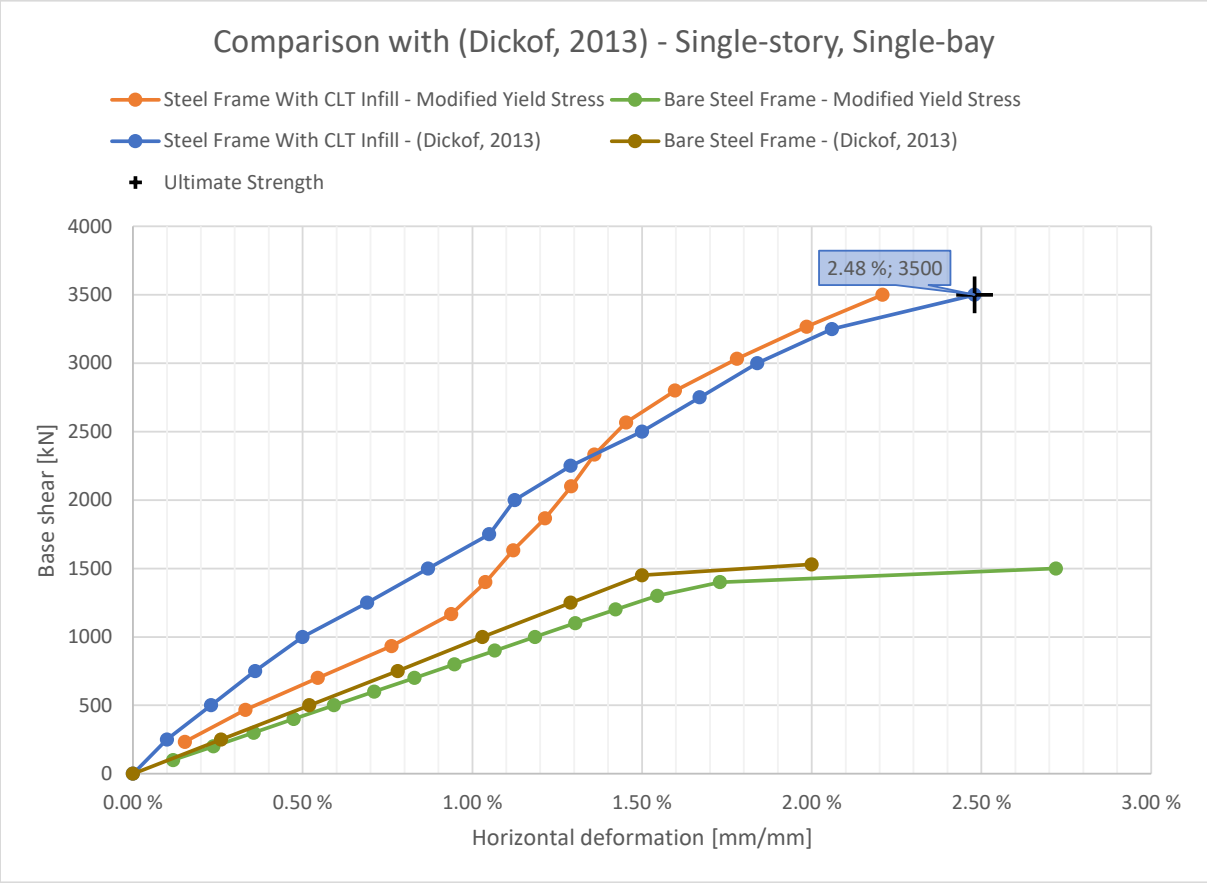

Figure 5.3: Comparison Between the Reference Model and the Model in (Dickof, 2013) With Modified Yield Stress

For the bare steel frame models, the similarity is now prominent. The bare steel frame in the reference model is still slightly less stiff; however, with the modified yield stress, both models now yield at a base shear of roughly 1400 kN.

Increasing the yield stress, the steel frame with CLT infill in the reference model undergoes a significant and long-lasting increase in stiffness after contact between the materials. The two models show similarity after contact, with the reference model gaining on and even overtaking the model in (Dickof, 2013) in terms of stiffness. The ultimate steel stress for the reference model with modified yield stress is not defined.

To clarify, no analysis utilizes the modified yield stress. Instead, it is solely presented to provide an alternative comparison with the model in (Dickof, 2013), accounting for the limitation discussed in 5.1.1.

5.4. Parametric Analyses

This section discusses the parameter adjustments and their effect on the results. In some cases, the effect of the adjustments can be anticipated. For example, it is expected that the stiffness of the system will increase as the thickness of the CLT panel increases. For such instances, the magnitude of the effect of the parameter adjustment is more compelling.

5.4.1. Frame Span

According to (Richards, 2017), the lateral stiffness of a moment-resisting frame is given by

$$k = \frac{\frac{24EI_c{}^2}{h^4} + \frac{144EI_cI_b}{h^3L}}{\frac{4I_c}{h} + \frac{6I_b}{L}} \tag{5.1}$$

Where:

k	is the stiffness
E	is the modulus of elasticity
I_c	is the column's second moment of inertia
I_b	is the beam's second moment of inertia
h	is the height of the frame
L	is the span of the frame

Examining equation (5.1), it is apparent that increasing the span of the frame reduces its stiffness. A higher span-to-height ratio results in more flexible frames that will experience more significant deformation. However, investigating Figure 4.4, it is evident that the larger frame spans are slightly stiffer before contact between the steel frame and CLT panel (up until 45 mm horizontal deformation). This deviation is due to the increased number of connectors along the width of the frame for the larger frame spans, as presented in Table 3.6.

According to (Richards, 2017), the lateral stiffness of a cantilever wall is given by

$$k = \frac{1}{\frac{h^3}{3EI} + \frac{1{,}2h}{AG}} \tag{5.2}$$

Where:

k	is the stiffness
E	is the modulus of elasticity
I	is the wall's second moment of inertia
h	is the height of the wall
A	is the area of the wall (length x height)
G	is the shear modulus

When the steel frame and CLT panel make contact at about 45 mm horizontal deformation, the stiffnesses increase at different rates. Equation (5.2) shows that the wall becomes stiffer by increasing the length and, subsequently, the area. The larger spans experience a more rapid increase in stiffness. At a base shear of 2500 kN, a reduction of 18,63% in horizontal deformation is registered when comparing case 3 to the reference model. As the panels begin to crush, all configurations lose stiffness and eventually reach their ultimate strengths.

The frame span substantially affects the base shear needed for the linear elastoplastic steel to reach its ultimate stress. Because the larger span configurations have a stiffer CLT panel, the steel frame carries a lesser portion of the load. As a result, an 11,9% increase in ultimate strength is registered when comparing case 1 to the reference model. For the larger frame spans, the ultimate strength is even higher.

An interesting observation is that increasing the frame span has less effect on the horizontal deformation as the spans get more extensive. To illustrate, Table 5.2 shows the effect of an increasing span at a base shear of 2500 kN.

Table 5.2: Effect of Increasing Frame Span at a Base Shear of 2500 kN

Configuration	Reference model	Case 1	Case 2	Case 3
Span	6 m	7 m	8 m	9 m
Horizontal deformation	102 mm	90 mm	85 mm	83 mm
Difference in mm*	-	-12 mm	-5 mm	-2 mm
Difference in percent*	-	-11,77%	-5,56%	-2,35%
*configuration_i – $\text{configuration}_{i-1}$				

Considering solely the deformation, one could argue that there is not a substantial benefit in increasing the frame span beyond a certain threshold. The cost and weight will rise, while the effect on the horizontal deformation will be minimally. On the other hand, the ultimate strength seems to increase drastically with the frame span. In earthquake-prone regions a high ultimate strength is necessary, and a larger frame span may prove to be advantageous.

5.4.2. Connection Spacing

As discussed in Section 5.35.2, the main contributors to the stiffness of the system, until it approaches a value just below 1% horizontal deformation, are the steel frame and the connectors. Figure 4.5 shows the effect of adjusting the maximum connection spacing. The configurations with reduced connection spacings are stiffer and yield slightly less horizontal deformation.

After the steel frame and CLT panel make contact at a value of just below 1% horizontal deformation, the difference in stiffness becomes more noticeable. The configurations with shorter connection spacing experience less deformation at equivalent base shears. At a base shear of 2500 kN, a reduction of 12,09% in horizontal deformation is registered when comparing case 1 to case 3 (smallest to largest maximum connection spacing). The difference in deformation remains roughly the same until the configurations reach their ultimate strengths.

It is recognizable that the curves of the reference model and case 2 in Figure 4.5 reveal a pattern of close following, even exhibiting synchronous motion at times. Another unexpected element of the results is the high ultimate strength of case 3. The abnormal behavior of some of the connection spacing configurations can be explained by the stress concentration and mesh size limitations discussed in Section 5.1.2.

Overall, the difference in stiffness is marginal, suggesting that adding or removing a couple of connectors along the edges of the panel has a minimal effect on the overall performance of the hybrid system.

5.4.3. Perforations in CLT Panel

As expected, Figure 4.6 shows that the perforations do not affect the stiffness of the hybrid system before contact between the steel frame and CLT panel. They will reduce the stiffness of the panel, but not enough to impact the initial performance of the hybrid system.

At a value of just below 1% horizontal deformation, the steel frame and CLT panel make contact, and the stiffness increases considerably. The stiffness decreases earlier and more rapidly for the more extensive perforation configurations, resulting in a magnifying difference in deformation as the base shear increases. For example, at a base shear of 2500 kN, an increase of 7,65% and 20% in horizontal deformation is registered when adding door and window perforations, respectively.

The ultimate strength of the configurations steadily reduces as perforations are added to the CLT panel. A decrease of 3,06% and 5,44% is registered when adding door and window perforations, respectively. Figure 4.7 and Figure 4.8 show the von Mises stress distribution in the panels with perforations. The decrease in the ultimate strength of the perforation configurations is modest because the panels still carry a significant portion of the load. When adding perforations, the stress distribution becomes more uniform across the panel.

Although the configurations with larger perforations have a lower ultimate strength, the effect is limited. However, perforations substantially affect the horizontal deformation of the hybrid system. Therefore, extra considerations should be given before adding too extensive perforations to the CLT panel for structures where limiting the horizontal deformation is crucial.

5.4.4. CLT Panel Thickness

As in Section 5.4.3, Figure 4.9 shows that the thickness of the CLT panel does not affect the initial performance of the hybrid system. The materials make contact at just below 1% horizontal deformation. At this point, the effect of the CLT panel thickness becomes evident. The thicker panels gain stiffness more rapidly, and the difference in deformation magnifies as the base shear increases. At a base shear of 2500 kN, a reduction of 21,62% in horizontal deformation is registered when comparing case 5 to case 1 (thickest to thinnest CLT panel).

The ultimate strength of the configurations increases with the thickness of the CLT panel. As the panel gets thicker, it gains stiffness and subsequently the ability to carry a more significant portion of the load. As a result, the steel frame now carries a lesser portion of the load and can reach higher base shears before achieving its ultimate stress. To illustrate, a 19,57% increase in ultimate strength is registered when comparing case 5 to case 1 (thickest to thinnest CLT panel).

Analogous to Section 5.4.1, increasing the thickness of the CLT panel has less effect on the horizontal deformation and the ultimate strength as the panels get thicker. Table 5.3 shows the effect of an increasing thickness at a base shear of 2500 kN.

Table 5.3: Effect of Increasing Thickness of CLT Panel at a Base Shear of 2500 kN

Configuration	Case 1	R.M.	Case 2	Case 3	Case 4	Case 5
Thickness [mm]	80	99	120	140	160	180
Horizontal deformation	1,85%	1,7%	1,6%	1,53%	1,49%	1,46%
Difference*		-0,15%	-0,1%	-0,07%	-0,04%	-0,03%
Difference in percent*		-8,11%	-5,88%	-4,38%	-2,61%	-2,01%
Ultimate strength	2810kN	2940 kN	3070 kN	3170 kN	3270 kN	3360 kN
Difference in kN*		130 kN	130 kN	100 kN	100 kN	90 kN
Difference in percent*		4,63%	4,42%	3,26%	3,16%	2,75%

*configuration_i – $\text{configuration}_{i-1}$

Examining Table 5.3, one could argue that there comes a point when increasing the thickness of the CLT panel offers negligible benefits. This is because the costs and weight of the panel will increase while the impact on horizontal deformation and ultimate strength will be minimal.

6. Conclusion

Adding a CLT panel to a steel frame significantly increases the stiffness and ultimate strength of the hybrid system. The CLT panel acts as a compression strut, carrying a substantial portion of the load and relieving the steel frame from this burden. Utilizing a CLT panel as an infill in a moment-resisting steel frame increases the ultimate strength of the system by 194%.

The parametric analysis of the frame span showed a reduced horizontal deformation and a significant increase in ultimate strength for larger span configurations. However, the effect on the horizontal deformation diminished as the spans became more extensive. The connection spacing parametric analysis altered the mesh size while retaining the geometry, yielding results that are hard to interpret and compare to one another. Nevertheless, for shorter connection spacings, the horizontal deformation seemed to slightly decrease. Incorporating perforations into the CLT panel increased the horizontal deformation and slightly reduced the ultimate strength of the hybrid system. The modest decrease in ultimate strength was attributed to the panel's continued ability to carry a significant portion of the load. Adding perforations resulted in a more uniform stress distribution across the panel. Increasing the thickness of the CLT panel resulted in a decrease in horizontal deformation and an increase in ultimate strength. As with the frame span, increasing the thickness of the CLT panel had less effect on the horizontal deformation as the panels got thicker. Novel to the parametric analysis of the panel thickness, the effect on the ultimate strength also diminished as the thickness of the panel increased.

The increased stiffness and strength of the hybrid system provide a significant improvement over conventional moment-resisting steel frames, enhancing the structural performance under seismic forces. CLT is a renewable and environmentally friendly construction material, contributing to reduced carbon emissions. Furthermore, the lightweight nature and high degree of prefabrication of CLT facilitate more accessible transportation and shorter construction schedules. This study affirms previous research, particularly the findings in (Dickof, 2013), which highlight the reduced horizontal deformation and increased ultimate strength that comes with infilling a moment-resisting steel frame with a CLT panel.

Overall, this study underscores the importance of investigating innovative solutions like CLT-steel hybrid shear walls to advance seismic design. This hybrid approach's improved performance and sustainability benefits highlight its potential for widespread implementation

as lateral force-resisting systems. As further research and development continue, these findings can pave the way for safer, more resilient structures in earthquake-prone regions.

6.1. Future Research

A suggested future work is to use surface-to-surface instead of point-to-point contact to mitigate the effect of the stress concentrations and mesh size limitations discussed in Section 5.1.2. According to (ANSYS, s.a.-d), CONTA174, which simulates contact between three-dimensional target surfaces, would be a fitting element.

In addition, it would be interesting to perform a cost and weight analysis, which would provide valuable insights and add an exciting dimension to the study. It would facilitate for concrete recommendations regarding the threshold beyond which increasing the frame span or the CLT panel thickness has no substantial benefits.

Moreover, an intriguing concept for future research would be exploring the possibility of rehabilitating and strengthening old moment-resisting steel frames with CLT infill. This investigation could contribute to developing practical and cost-effective retrofit solutions incorporating sustainable and renewable construction materials.

Finally, adding more stories and bays to the existing model would provide a broader range of results that could be compared to existing studies, contributing to a more comprehensive understanding of the hybrid system.

References

ANSYS [Computer software]. (2022). *ANSYS 2022 R1*. Canonsburg, PA.

ANSYS, I. (s.a.-a). *BEAM189*. Available at: https://www.mm.bme.hu/~gyebro/files/ans_help_v182/ans_elem/Hlp_E_BEAM189.html (accessed: 25.04.2023).

ANSYS, I. (s.a.-b). *COMBIN39*. Available at: https://www.mm.bme.hu/~gyebro/files/ans_help_v182/ans_elem/Hlp_E_COMBIN39.html (accessed: 19.04.2023).

ANSYS, I. (s.a.-c). *COMBIN40*. Available at: https://www.mm.bme.hu/~gyebro/files/ans_help_v182/ans_elem/Hlp_E_COMBIN40.html (accessed: 22.04.2023).

ANSYS, I. (s.a.-d). *CONTA174*. Available at: https://www.mm.bme.hu/~gyebro/files/ans_help_v182/ans_elem/Hlp_E_CONTA174.html (accessed: 12.05.2023).

ANSYS, I. (s.a.-e). *SOLSH190*. Available at: https://www.mm.bme.hu/~gyebro/files/ans_help_v182/ans_elem/Hlp_E_SOLSH190.html (accessed: 25.04.2023).

Bhat, P. (2013). *Experimental investigation of connection for the FFTT, a timber-steel hybrid system*: University of British Columbia.

Dickof, C. (2013). *CLT infill panels in steel moment resisting frames as a hybrid seismic force resisting system*: University of British Columbia.

Enso, S. (s.a.). *Cross-laminated timber (CLT)*. Available at: https://www.storaenso.com/en/products/mass-timber-construction/building-products/clt (accessed: 17.04.2023).

Horx-Strathern, O., Varga, C. & Guntsching, G. The Future of Timber Construction CLT—Cross Laminated Timber, A Study about Changes, Trends, and Technologies of Tomorrow. *A Study in Collaboration with Stora Enso*.

Jeleč, M. & Rajčić, V. (2018). Cross-laminated timber (CLT)–a state of the art report. *Građevinar*, 70 (02.): 75-95.

Khajehpour, M. (2020). *Numerical Study on the Seismic Performance of Hybrid Steel Moment Frames with CLT Balloon Shear Walls*: University of Northern British Columbia.

Khorasani, Y. (2011). *Feasibility study of hybrid wood steel structures*: University of British Columbia.

Lehmann, S. (2012). Sustainable construction for urban infill development using engineered massive wood panel systems. *Sustainability*, 4 (10): 2707-2742.

Moelven. (s.a.). *KL-tre (massivtre)*. Available at: https://www.moelven.com/no/no/limtre/kl-tre-massivtre/ (accessed: 18.04.2023).

Norge, S. (2005). *Eurokode 3: Prosjektering av stålkonstruksjoner. Del 1-1: Allmenne regler og regler for bygninger (NS-EN 1993-1-1:2005+NA:2008)*: Standard Norge.

Quintana Gallo, P. & Carradine, D. (2018). State of the art of timber-based hybrid seismic-resistant structures. *BRANZ Study Report SR400, Judgeford, New Zealand*.

Resmi, R. & Roja, S. Y. (2016). A review on performance of shear wall. *International Journal of Applied Engineering Research*, 11 (3): 369-373.

Richards, P. W. (2017). *Seismic Principles*: CreateSpace Independent Publishing Platform.

Schneider, J. (2009). *Connections in Cross-Laminated-Timber Shear Walls Considering the Behaviour under Monotonic and Cyclic Lateral Loading*. MASc Thesis. Stutgart, Germany: University of Stutgart.

Slavid, R. (2005). *Wood Architecture*: Laurence King.

SteelConstruction.info. (s.a.). *The case for steel*. Available at: https://steelconstruction.info/The_case_for_steel#cite_ref-No2_2-0 (accessed: 17.04.2023).

Stiemer, S., Tesfamariam, S., Karacabeyli, E. & Propovski, M. (2012). *Development of steel-wood hybrid systems for buildings under dynamic loads*. Proceedings of the 7th International Specialty Conference on Behavior of Steel Structures in Seismic Areas (STESSA), Santiago, Chile.

Tesfamariam, S., Stiemer, S. F., Dickof, C. & Bezabeh, M. A. (2014). Seismic Vulnerability Assessment of Hybrid Steel-Timber Structure: Steel Moment-Resisting Frames with CLT Infill. *Journal of Earthquake Engineering*, 18 (6): 929-944. doi: 10.1080/13632469.2014.916240.

Vogiatzis, T., Tsalkatidis, T. & Avdelas, A. (2019). Steel framed structures with cross laminated timber infill shear walls and semi-rigid connections. *Int. J. Eng*, 8: 433-443.

Vogiatzis, T., Tsalkatidis, T. & Efthymiou, E. (2022). The wall–frame interaction effect in CLT-steel hybrid systems. *Frontiers in Built Environment*, 8. doi: 10.3389/fbuil.2022.1008973.

Young, W. C., Budynas, R. G. & Sadegh, A. M. (2012). *Roark's formulas for stress and strain*. 8th ed.: The McGraw-Hill Companies, Inc.

Appendices

Appendix A Data Points for COMBIN39-Element

Table A-1: Data Points for COMBIN39-element

Force [kN]	Displacement [mm]
0	0
12,5	5
20	15
25	30
7,5	70

Appendix B Steel Frame Cross-Sections

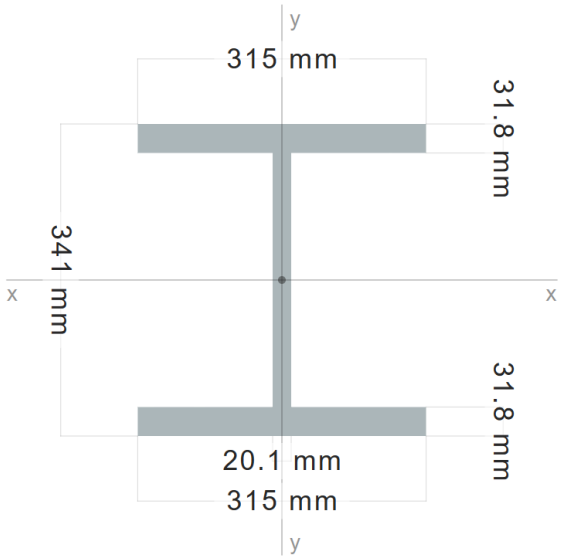

Figure B-1: W310x202 Cross-Section

Source: Blue Ketchep. (s.a.). *CA – W310x202.* Available at: https://sections.app/section/uJKoy-LZQoaP57Z4fAyz6Q/W310x202 (accessed: 02.05.2023).

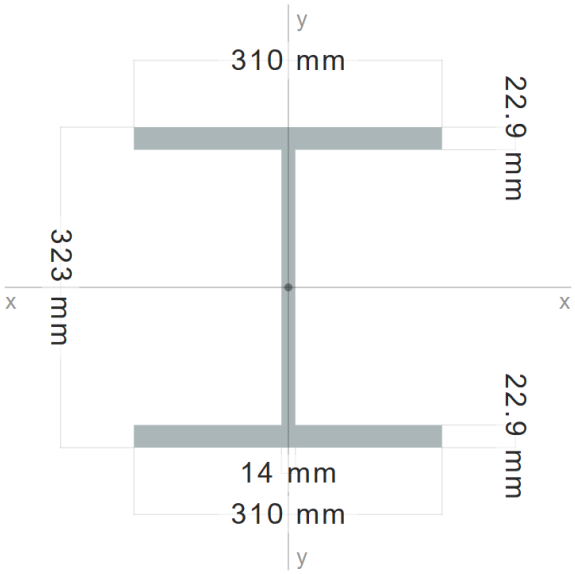

Figure B-2: W310x143 Cross-Section

Source: Blue Ketchep. (s.a.). *US – W310x143.* Available at: https://sections.app/section/MVxr3CXXrEmtMXV4-KRB0Q/W310X143 (accessed: 02.05.2023).

Appendix C Stress Distribution for Parametric Analyses

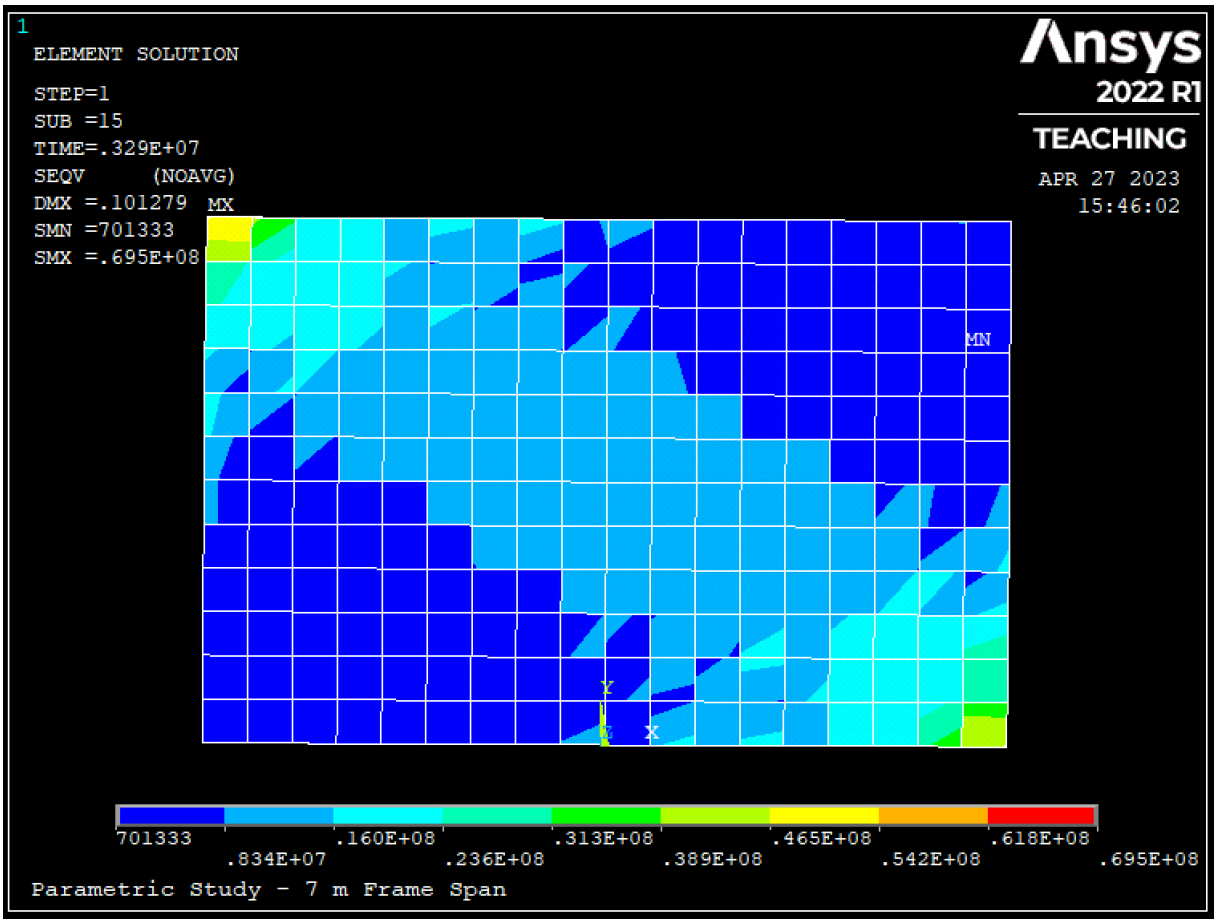

Figure C-1: Von Mises Stress Distribution in CLT Panel – 7 m Frame Span

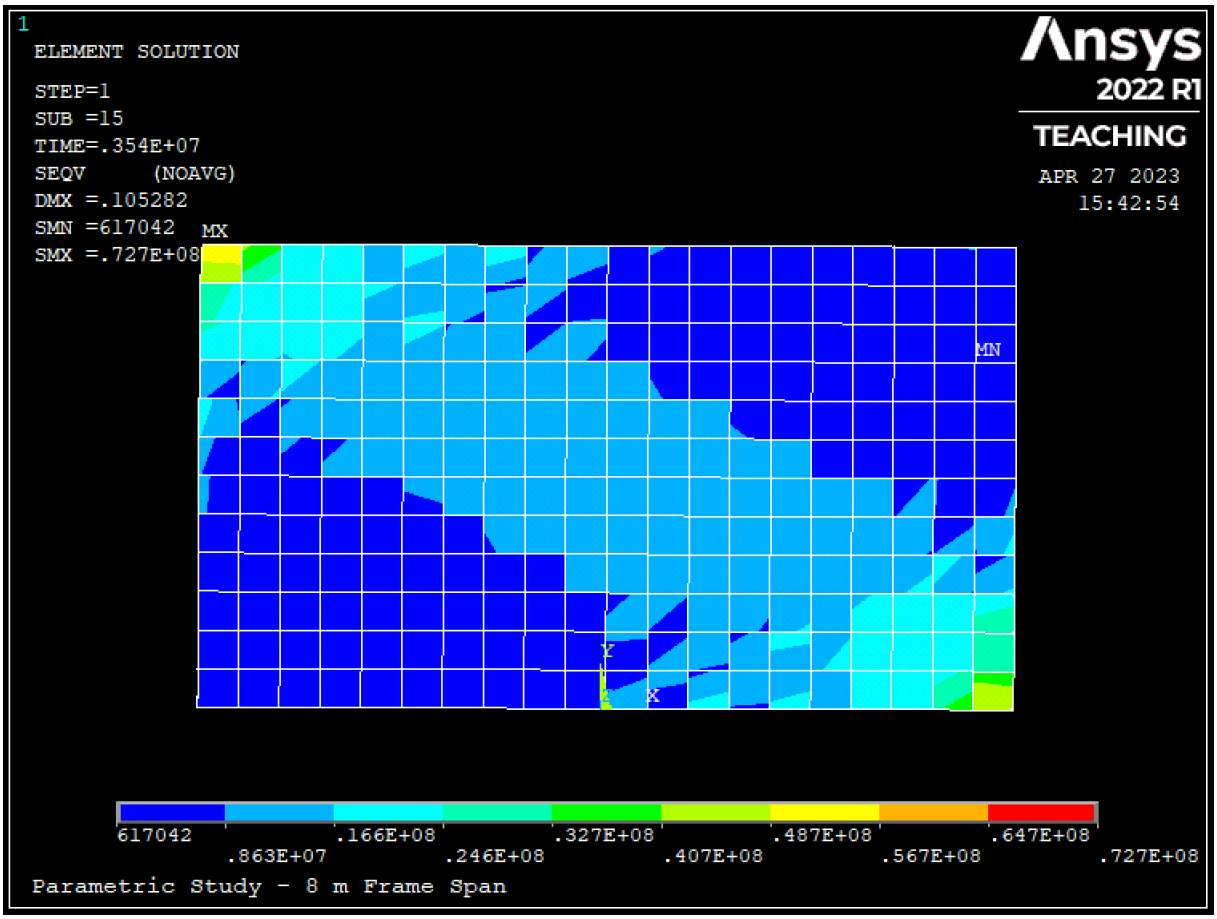

Figure C-2: Von Mises Stress Distribution in CLT Panel – 8 m Frame Span

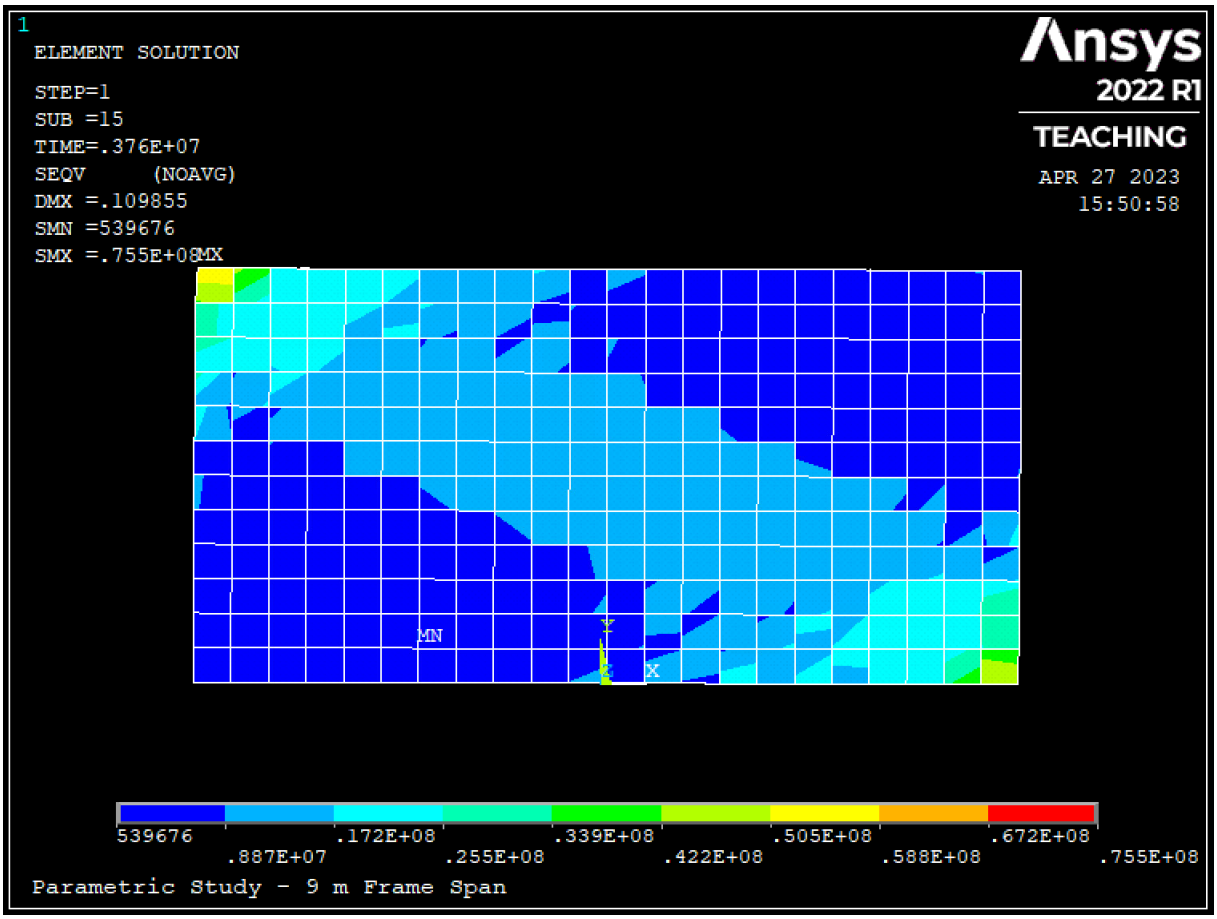

Figure C-3: Von Mises Stress Distribution in CLT Panel – 9 m Frame Span

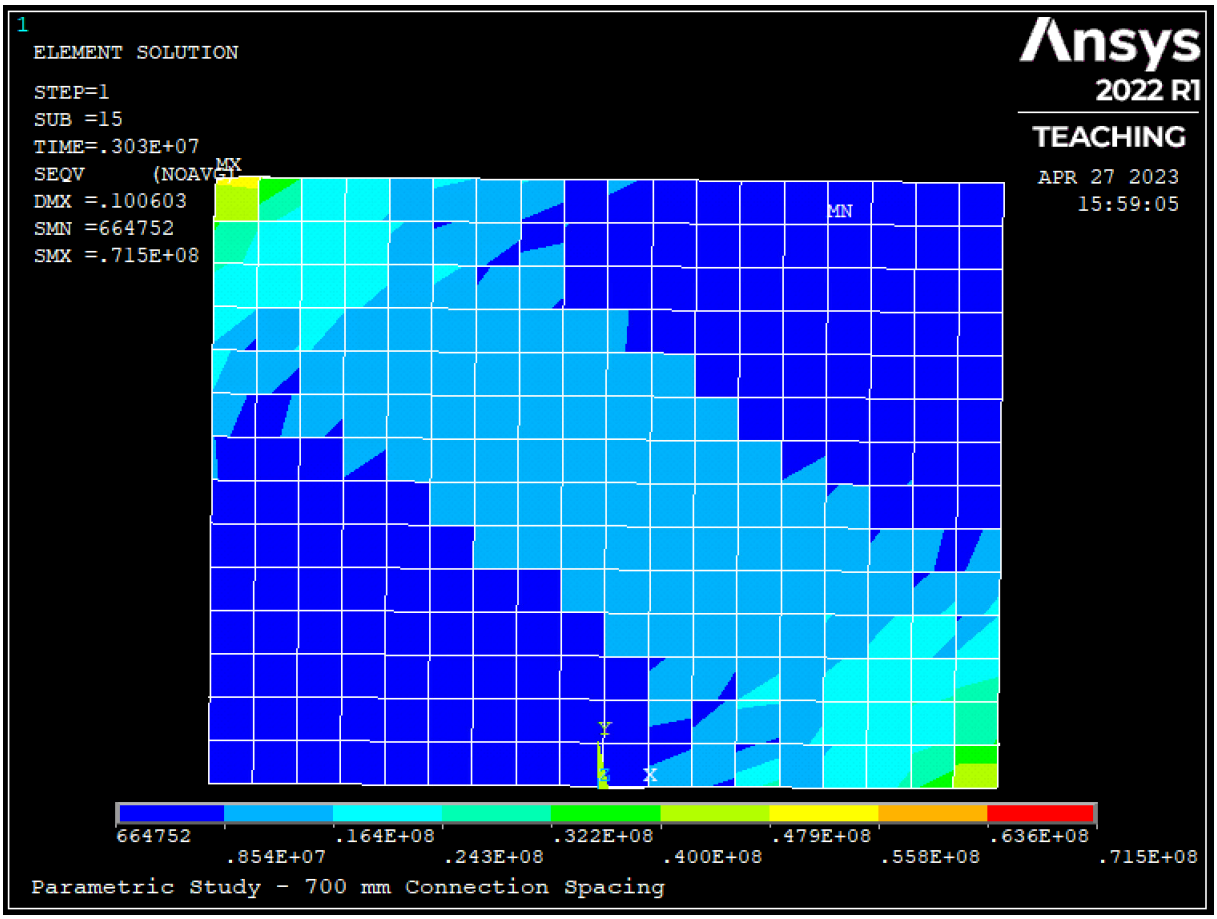

Figure C-4: Von Mises Stress Distribution in CLT Panel – 700 mm Connection Spacing

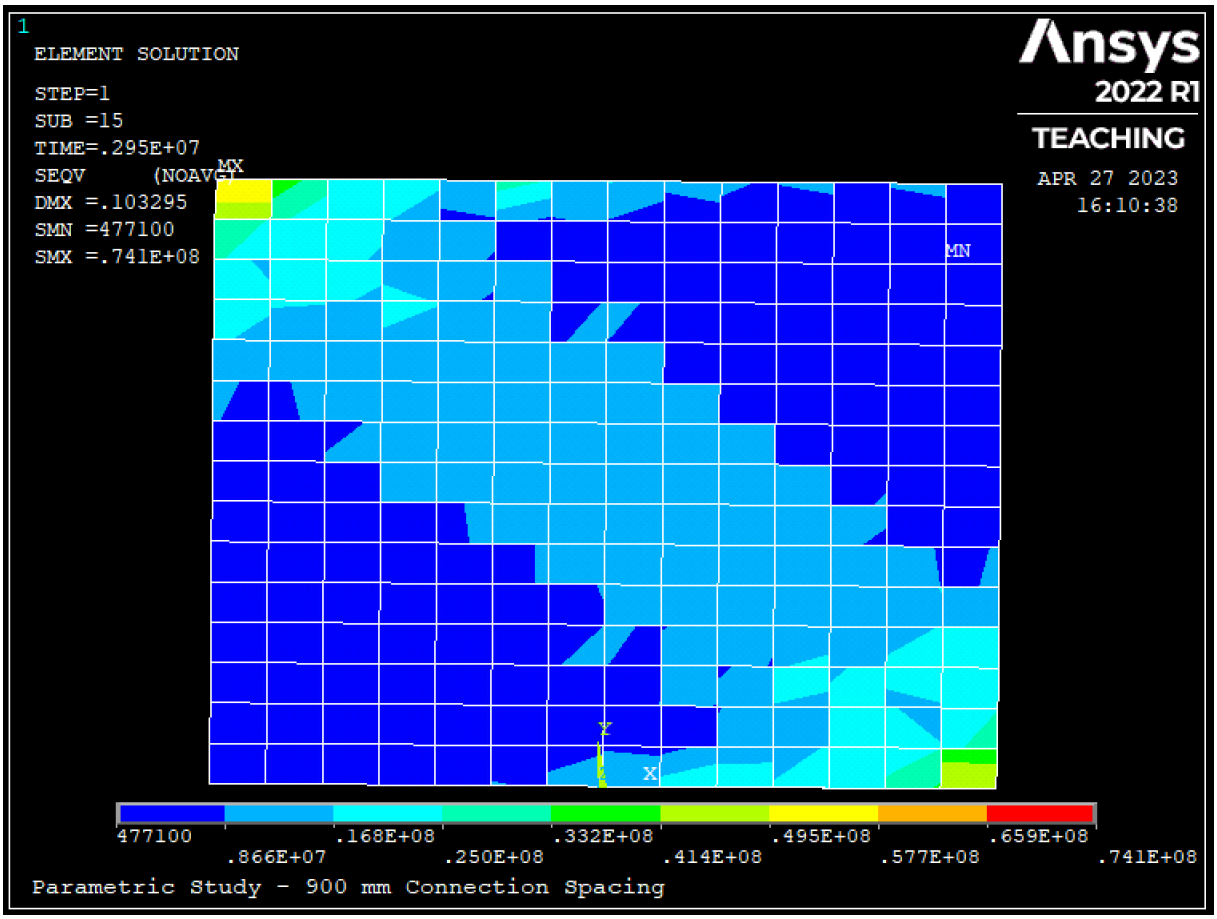

Figure C-5: Von Mises Stress Distribution in CLT Panel – 900 mm Connection Spacing

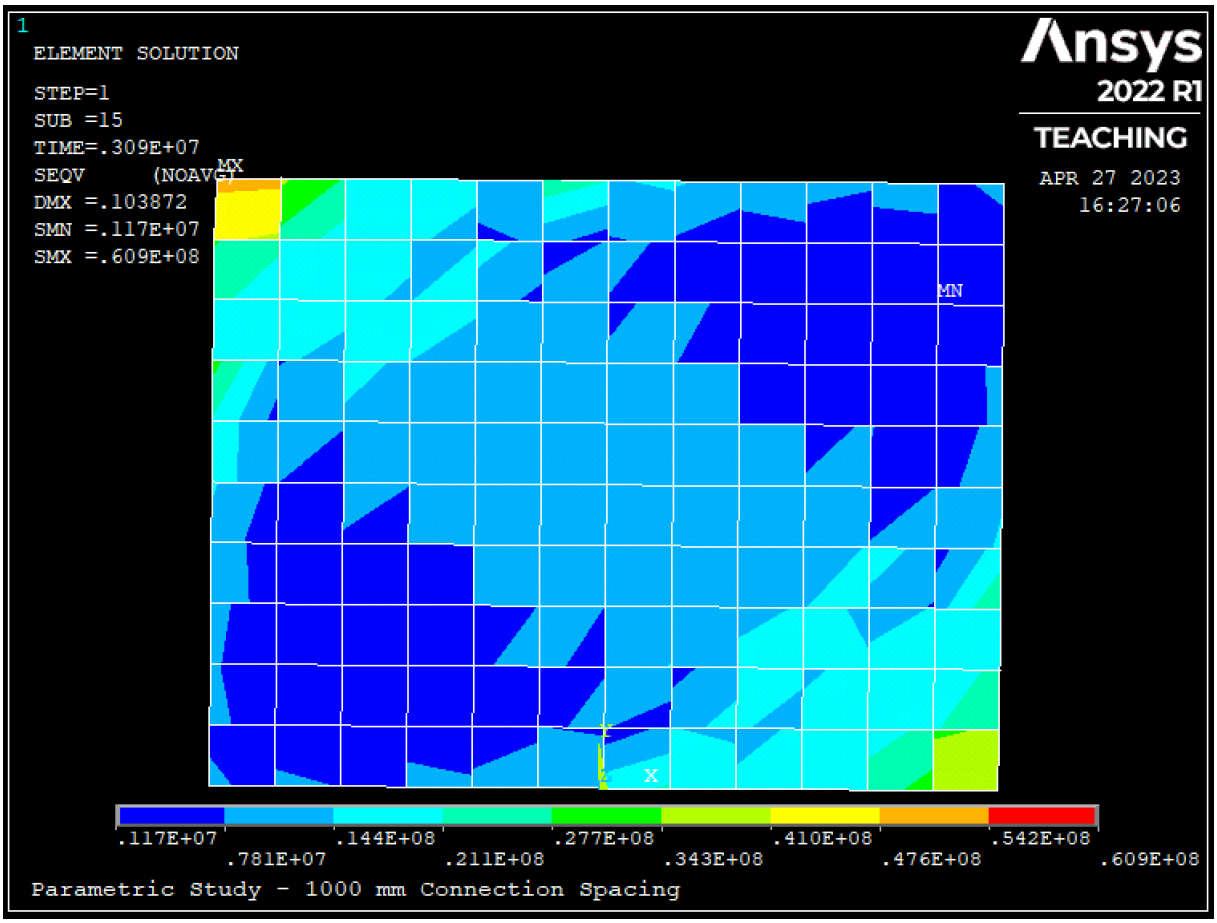

Figure C-6: Von Mises Stress Distribution in CLT Panel – 1000 mm Connection Spacing

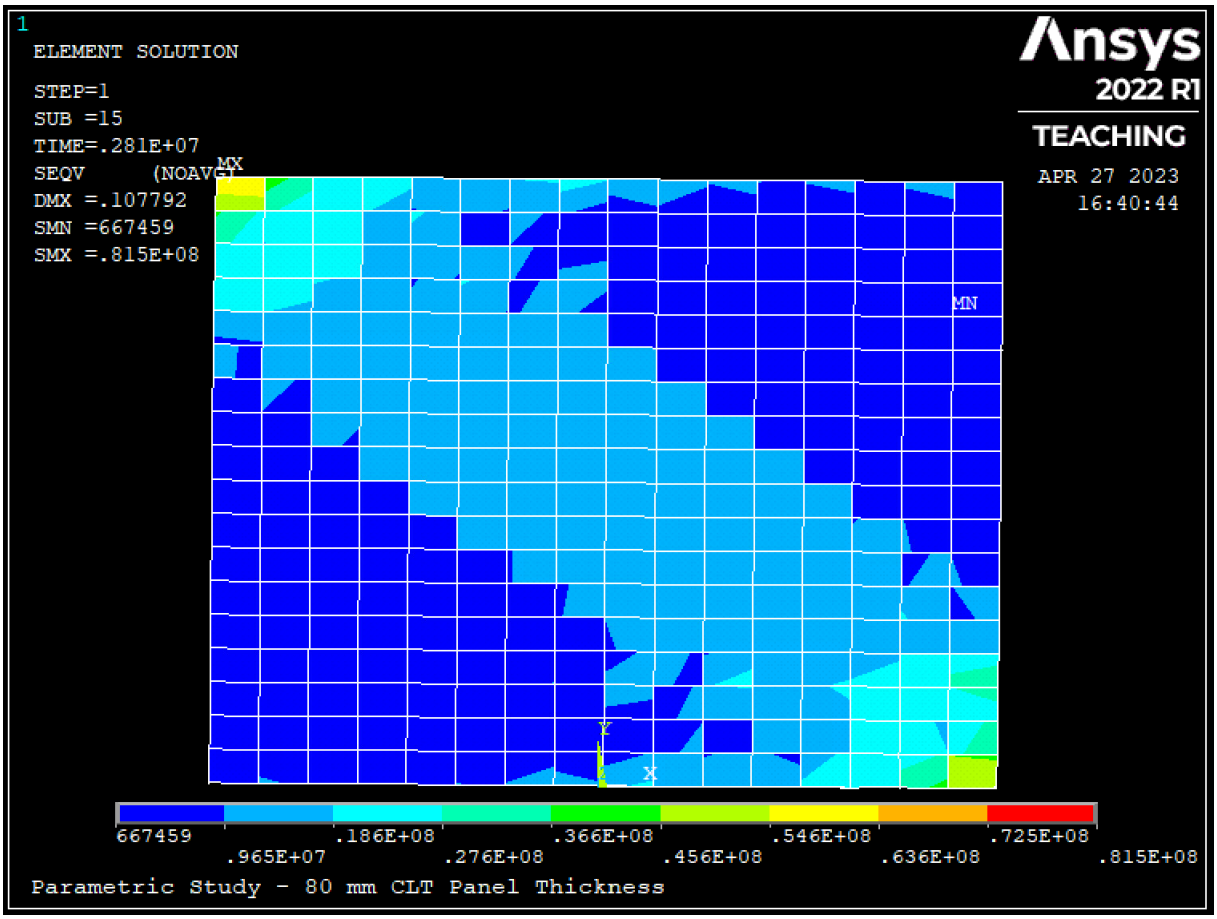

Figure C-7: Von Mises Stress Distribution in CLT Panel – 80 mm CLT Panel Thickness

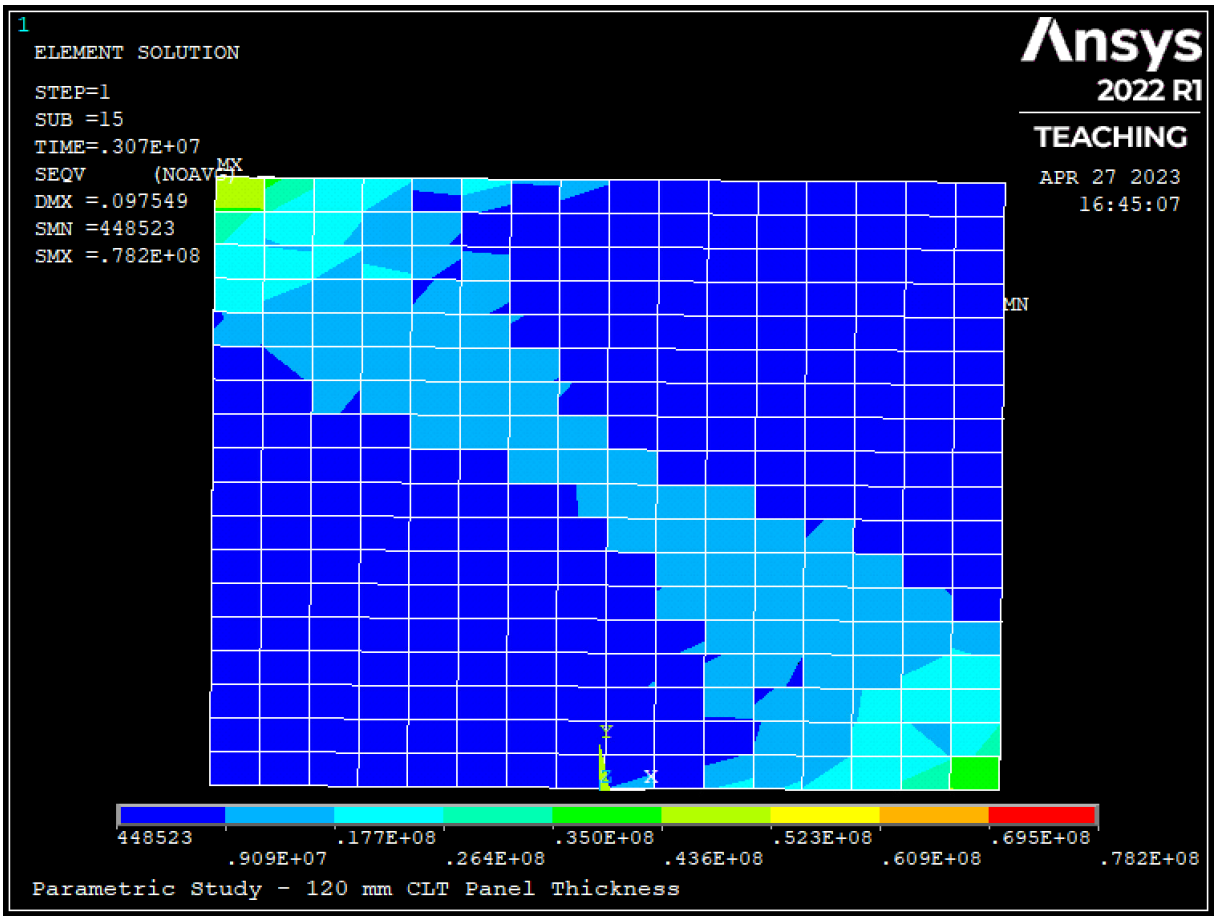

Figure C-8: Von Mises Stress Distribution in CLT Panel – 120 mm CLT Panel Thickness

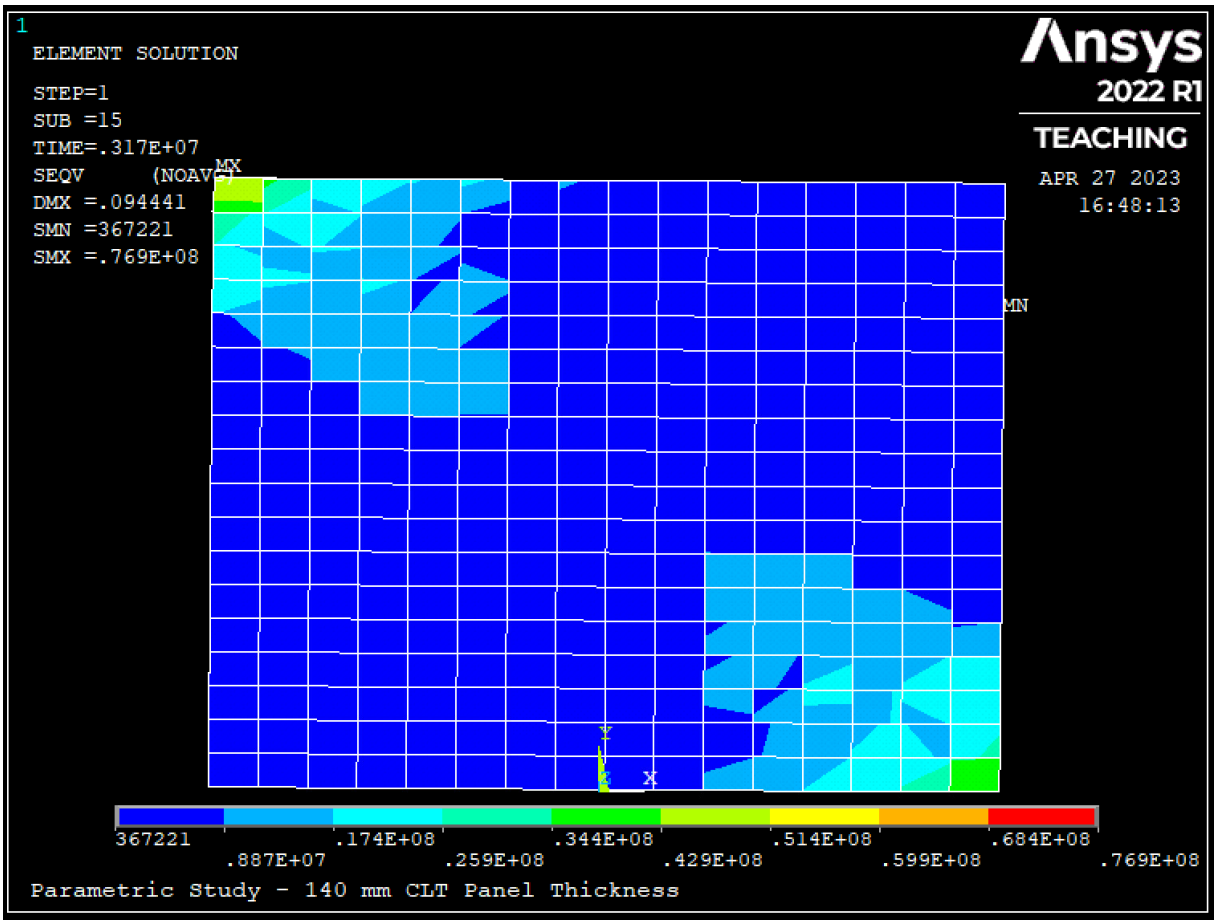

Figure C-9: Von Mises Stress Distribution in CLT Panel – 140 mm CLT Panel Thickness

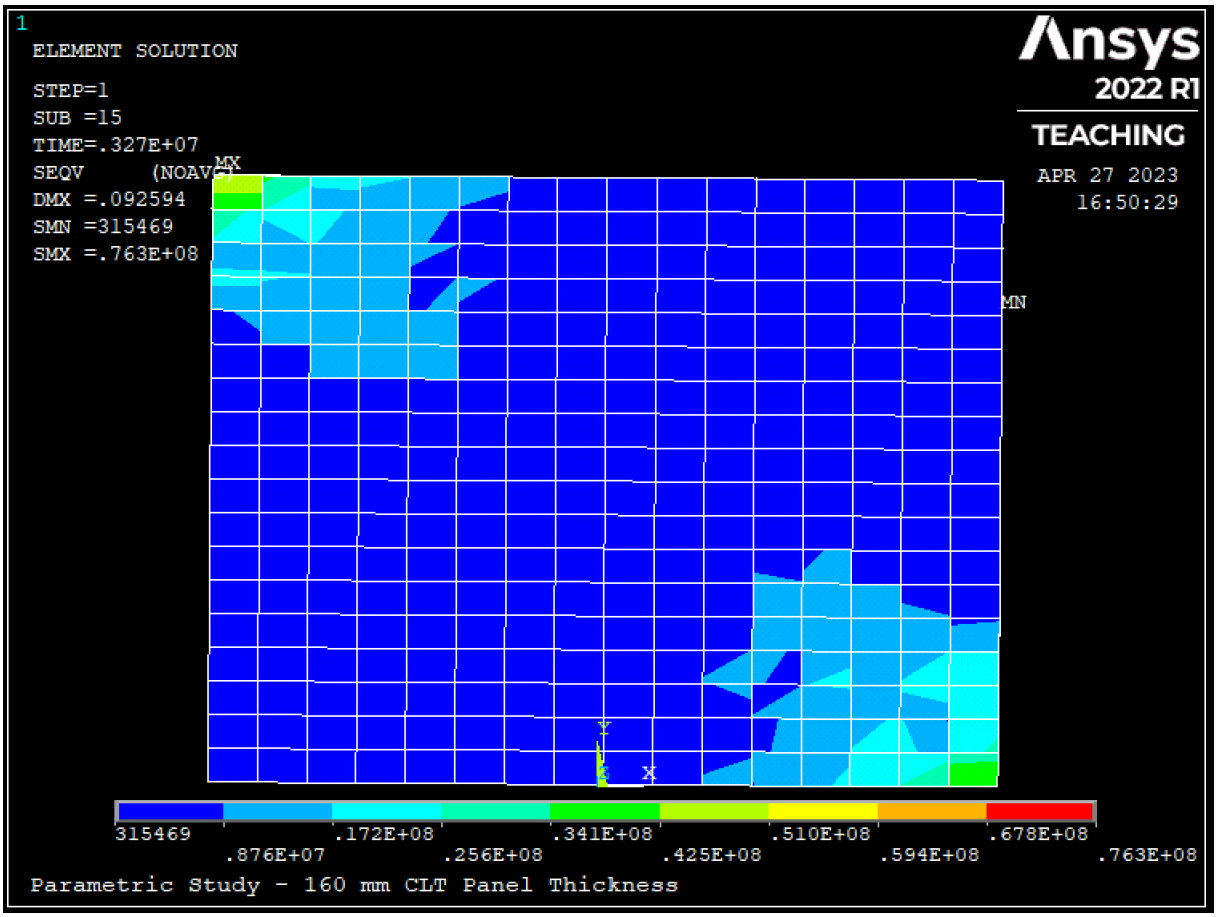

Figure C-10: Von Mises Stress Distribution in CLT Panel – 160 mm CLT Panel Thickness

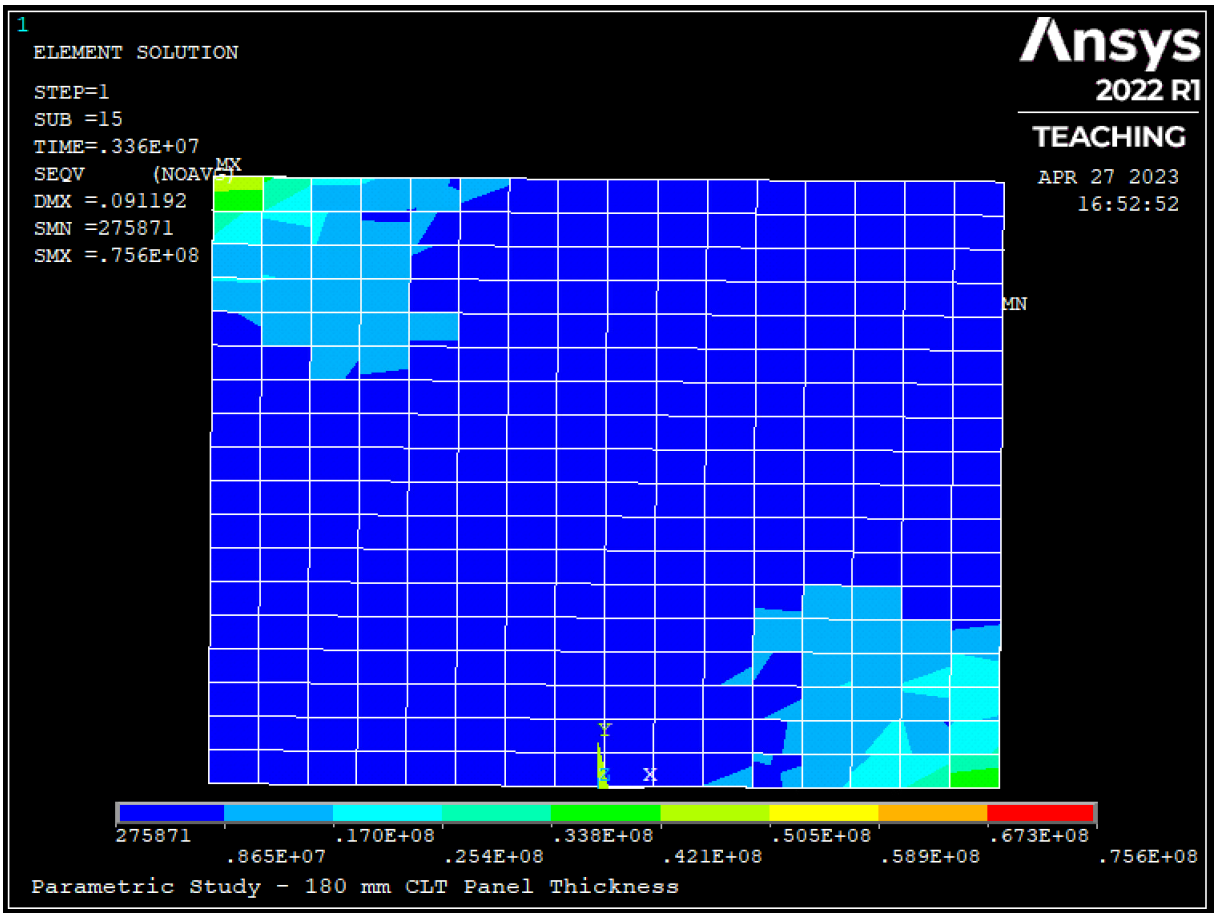

Figure C-11: Von Mises Stress Distribution in CLT Panel – 180 mm CLT Panel Thickness

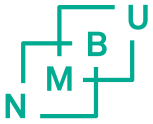

Norges miljø- og biovitenskapelige universitet
Noregs miljø- og biovitskapelege universitet
Norwegian University of Life Sciences

Postboks 5003
NO-1432 Ås
Norway